NACA TN 3929 10277

TECH LIBRARY KAFB, NM
0067133

# NATIONAL ADVISORY COMMITTEE FOR AERONAUTICS

TECHNICAL NOTE 3929

## A GENERAL SYSTEM FOR CALCULATING BURNING RATES OF PARTICLES AND DROPS AND COMPARISON OF CALCULATED RATES FOR CARBON, BORON, MAGNESIUM, AND ISOOCTANE

By Kenneth P. Coffin and Richard S. Brokaw

Lewis Flight Propulsion Laboratory
Cleveland, Ohio

Washington
February 1957

AFMDC
TECHNICAL LIBRARY
AFL 2811

TECH LIBRARY KAFB, NM
0067133



4076

TABLE OF CONTENTS

| | Page |
|---|---|
| SUMMARY | 1 |
| INTRODUCTION | 2 |
| GENERAL EQUATIONS | 3 |
| APPLICATION OF EQUATIONS | 11 |
| Carbon | 11 |
| Numerical integration | 12 |
| Analytical solution | 16 |
| Boron | 19 |
| Hydrocarbons | 19 |
| Magnesium | 20 |
| RESULTS | 20 |
| SUMMARY OF RESULTS | 23 |
| APPENDIXES | |
| A - SYMBOLS | 24 |
| B - DETAILS OF BORON TREATMENT | 27 |
| General Boron System with Gaseous $B_2O_3$ | 27 |
| Condensed $B_2O_3$, a Special Boundary Condition | 29 |
| Burning Rate and Flame Structure | 32 |
| Graphical Method for Burning Rate | 33 |
| C - REDUCTION OF GENERAL EQUATIONS TO SIMPLIFIED EQUATIONS | 35 |
| Hydrocarbons and Boron | 35 |
| Magnesium | 37 |
| D - DERIVATION OF APPROXIMATE DIFFUSION EQUATIONS FOR MULTICOMPONENT MIXTURES | 41 |
| E - ESTIMATION OF $\delta_1$ FOR CARBON AND BORON COMBUSTION | 44 |
| REFERENCES | 46 |
| TABLES | |
| I - COMPUTED BURNING RATES OF VARIOUS SUBSTANCES | 47 |
| II - EFFECTS OF AMBIENT TEMPERATURE AND AMBIENT PARTIAL PRESSURE OF OXYGEN ON BURNING RATE OF BORON | 47 |

NATIONAL ADVISORY COMMITTEE FOR AERONAUTICS

TECHNICAL NOTE 3929

# A GENERAL SYSTEM FOR CALCULATING BURNING RATES OF PARTICLES AND DROPS AND COMPARISON OF CALCULATED RATES FOR CARBON, BORON, MAGNESIUM, AND ISOOCTANE

By Kenneth P. Coffin and Richard S. Brokaw

## SUMMARY

A system with general equations has been devised for computing the burning rates of small particles burning as diffusion flames; the equations account for the effects of diffusion and dissociation with a high degree of rigor. Two types of solutions are carried out: (1) a numerical integration of considerable complexity, and (2) a somewhat less complicated and less rigorous analytical solution involving stepwise iteration across the temperature profile. The direct results of the calculation are partial pressures as a function of temperature. Simple additional calculations produce the burning rate and the flame structure.

Both solutions were obtained for carbon burning in air; the differences are slight. For boron, because of the greater number of equilibria involved, only the analytical solution was undertaken; a special treatment for a solid reaction product, boric oxide ($B_2O_3$), was required. A number of ambient temperatures and ambient oxygen concentrations were examined in the case of boron; as an example, three graphs rapidly yield burning rates for a wide range of ambient conditions.

The general equations presented here reduce to the much simpler equations used by previous investigators. The simplified equations were also applied to boron, and yielded results in general agreement with the more detailed analytical solutions. Earlier results from the simplified equations for isooctane and magnesium are included for comparison. The simplified equations appear to be sufficiently accurate for many purposes.

For a series of substances covering a wide range of volatility, relative heat-release rates are in the order: hydrocarbon > magnesium > carbon ≅ boron.

## INTRODUCTION

In the last few years, a number of articles have appeared which treat the combustion of single fuel particles in quiescent air. The treatments of these diffusion flames vary in generality and in specific approach (refs. 1 to 6). They involve physical and mathematical approximations which are qualitatively acceptable, but which may introduce significant quantitative errors.

The general success of the stagnant-film treatment for the combustion of single liquid drops has tended to support the validity of the assumptions involved. The model assumes a steady-state diffusion flame surrounds the fuel drop. Oxygen diffuses inward, fuel vaporizes and diffuses outward, and they meet and react in a flame front symmetrically surrounding the drop; sufficient heat is conducted inward from the reaction zone to vaporize the fuel and heat the vapor to reaction temperature, while the remaining heat is conducted outward and, in part, is used to preheat the inbound oxygen. The reaction products diffuse outward.

The assumption of a diffusion flame mechanism with the over-all process controlled by the physical processes of heat conduction and diffusion carries the implicit assumption that the chemical processes within the flame front are fast. Such assumptions are in contrast to those made in considering ignition delay, in which chemical processes are presumed to control. In the case of flame speed, as well as in quenching-distance and dead-space phenomena, both chemical and physical processes are presumed to be involved. In the steady-state burning of a liquid monopropellant drop, a diffusion flame is not present, and both physical and chemical processes contribute to the over-all rate.

On the basis of the diffusion-flame (stagnant-film) model, burning rates in reasonable agreement with experiment have been calculated by many workers, although certain difficulties appear in the case of calculated flame structures. The main difficulty is that computed flame diameters are significantly greater than those observed experimentally; however, appropriate corrections involving the experimental boundary conditions result in only relatively small changes in the burning rate.

The general objective of this investigation was a more careful solution of the burning-rate problem in an effort to determine the limitations of the simpler treatments. More specifically, this investigation was concerned with the calculation of the relative burning rates for several solid combustibles representing a wide range of volatilities.

It seemed appropriate to make efforts to extend the calculations made on liquid fuels and carbon (refs. 1 and 5) to systems of solid combustibles which do not involve conventional fuels. The combustion of magnesium had been treated experimentally and a tentative approach to

4076

the theoretical treatment given (ref. 6). Magnesium is a combustible metal of relatively low volatility (b.p., 1393° K) and as such represents a transition to the less-volatile metals. For the present treatment, boron (b.p., 2550° K) was selected as a typical high-boiling-point combustible.

In this report, expressions for diffusion and heat conduction, as they apply to burning particles, are developed into a system of generalized equations somewhat along the lines indicated by Spalding in his approximate treatment of carbon (ref. 1). These equations are applied to boron and carbon, and they are reduced to the simpler equations used in the treatment of hydrocarbons and magnesium. The simplified equations are also applied to boron.

The general equations are developed in the next section. In the section following that development, carbon is considered as a detailed specific example of the use of the general equations. Carbon is treated in two ways, in terms of an exact numerical integration and in terms of a simpler analytical solution involving certain average values and limiting forms of the diffusion equations.

The boron system involves a more complex series of equilibria than that of the carbon system; therefore, only the analytical solution was undertaken. These results for boron are in turn compared with those obtained for boron by the simpler equations of the form used for isooctane (refs. 1 and 5) and magnesium (ref. 6). The details of the boron case are in appendix B. The general equations are reduced to the simpler equations for isooctane and magnesium in appendix C. The burning rates and particle lifetimes of carbon, magnesium, boron, and isooctane are compared.

## GENERAL EQUATIONS

The development in this section deals with the application of the equations for the conservation of mass, the conservation of energy, diffusion, heat conduction, and chemical equilibrium to the diffusion flame surrounding a burning particle or drop (fig. 1). In part, it is an extension of the early work of Spalding (ref. 1). In this section the equations are presented in general terms; in the following section, the burning of carbon is treated as a specific example of these general expressions. Equations are designated so that numbers in this section, the next section, and appendixes B and C apply to corresponding equations.

The general physical model is indicated in figure 1. The diffusion flame symmetrically surrounding the fuel particle may be divided into arbitrary zones for descriptive purposes and approximate calculations; the boundaries of the zones are indicated by concentric circles.

4076

CE-1 back

Convection is assumed to be absent. The central crosshatched portion represents the fuel; C represents the boundary with the ambient atmosphere. B (fig. 1(a)) or the region BB' (fig. 1(b)) represents the flame front, of infinitesimal or finite width, respectively; only diffusion occurs in the finite flame front. Chemical reaction rates are assumed to be fast relative to heat and mass transfer. In the region AB, sufficient heat is conducted inward to vaporize the fuel and raise it to the flame temperature; fuel is vaporized at the fuel surface A and diffuses to the flame front. In the regions BC or B'C, outside the flame front, the heat of combustion is dissipated outward by conduction, the reaction products diffuse out, and oxygen diffuses in, with an exchange of enthalpy between them. All these processes occur in a stagnant film. The ambient atmosphere is a source of oxygen and a sink for heat and combustion products.

4076

One of the major advantages of the equations presented in this section is that the artificial zones described above are eliminated. This in turn eliminates the arbitrary assignment of flame-front boundary conditions. Of course, other assumptions are introduced, for example, the existence of equilibrium throughout the system. Further, a more rigorous treatment of diffusion can be employed, although difficulties exist with the extrapolation of diffusion constants and thermal conductivities to high temperatures.

The equations required may be developed in the following manner. (Carbon, as a specific example of the general equations, is treated in the next section; boron is treated in detail in appendix B.) X,Y,Z, . . . are the $s$ atom species present in the system; fuel or oxidant or both may contain several species. For example, for carbon burning in air, carbon, oxygen, and nitrogen are $s = 3$ atom species. $X_{k_i}Y_{l_i}Z_{m_i}$ . . . is the $i^{th}$ species of the $\nu$ molecular species present ($k_i$, $l_i$, $m_i$, . . . = 0, 1, 2, 3, . . .). For example, in the carbon and air case, if the $i^{th}$ species is the carbon dioxide molecule, $C_1O_2N_0$ represents $CO_2$ with $k_{CO_2} = 1$, $l_{CO_2} = 2$, and $m_{CO_2} = 0$. (Symbols are defined in appendix A.)

For the conservation of mass, there is a continuity equation for each of the $s$ atom species; in terms of the total mass-transfer rate $W_i = W_{X_{k_i}Y_{l_i}Z_{m_i}}$, in moles per second, for each of the molecular species across any symmetrical surface around the particle, these equations are

4076

$$\left.\begin{aligned} W_X &= \sum_{i=1}^{i=\nu} k_i W_i = k_f W_f \\ W_Y &= \sum_{i=1}^{\nu} l_i W_i = l_f W_f \\ W_Z &= \sum_{i=1}^{\nu} m_i W_i = m_f W_f \end{aligned}\right\} \tag{1}$$

where $W_f$ is the burning rate of the fuel in moles per second. The coefficient of $W_f$ appropriate for each equation is determined by the composition of the fuel molecule $f = X_{k_f} Y_{l_f} Z_{m_f}$.

For systems with gaseous combustion products, there is a net outward flow of fuel $W_f$, because the drop is a fuel source; further, the net flow of oxidant and diluent gas from the ambient atmosphere is zero, because there is no sink in the system. The presence of some atom species both in the atmosphere and in the fuel (e.g., oxygen, when alcohol burns in air) is provided for in the equations. Should a combustion product stick on the surface or dissolve in the fuel, a sink would then exist; the coefficient of $W_f$ for the atom species involved in such a product would be negative and determined by the stoichiometry.

The diffusion equations for the problem involve certain approximations which are treated in appendix D. This treatment introduces approximations which are less severe than those made in the previous treatment of such problems. The diffusion equation for the $i^{th}$ molecular species is given by

$$-G_i = \frac{D_i}{RT}\frac{dp_i}{dr} + \frac{p_i}{p_{N_2}}\sum_{j=1}^{\nu-1}\frac{D_j}{RT}\frac{dp_j}{dr} = -\frac{W_i}{4\pi r^2} \qquad j \neq N_2 \text{ and } i \neq N_2 \tag{2a}$$

(eq. (D5) in appendix D). For the case of large fractions of inert gas, $p_i \rightarrow 0$. Then as in equation (D7)

$$-G_i = \frac{D_i}{RT}\frac{dp_i}{dr} = -\frac{W_i}{4\pi r^2} \qquad i \neq N_2 \tag{2b}$$

Similar equations are obtained for $\nu - 1$ molecular species. If the entire process occurs at constant pressure, the partial pressure of the inert gas is given by

$$p_{N_2} = P - \sum_{i \neq N_2}^{\nu} p_i \tag{3}$$

If no inert gas is present, the equations (2a) must be revised in terms of equations (D4) including the term $\frac{p_i}{p_\nu} G_\nu$ with some convenient reacting species designated as the $\nu^{th}$ species. If more than one inert gas is present, equations (2a) present no difficulty; however, when the continuity equation $W_{inert} = 0$ is used, equations (2b) indicate that the partial pressure of such an inert gas is constant and equal to the partial pressure in the boundary condition. 4076

In addition, there are equilibrium equations for $\nu - s$ molecular species (i.e., number of molecular species minus number of atom species). The $\nu - s$ equilibrium equations are written in terms of $\bar{s}$ molecular species where $\bar{s}$ equals $s$ minus the number of inert species. The $\bar{s}$ independent molecular species are usually selected for convenience as those noninert species having the highest partial pressures (however, they must represent all noninert atom species). A balanced chemical equation for the $i^{th}$ dependent species in terms of each ($g^{th}$) of the $\bar{s}$ independent species can be written

$$i + \sum_{g=1}^{\bar{s}} n_g g = 0 \tag{4}$$

where the $n_g$'s are the stoichiometric coefficients. Then

$$p_i = k_i \prod_{g=1}^{\bar{s}} p_g^{-n_g} \tag{5}$$

where

$$\log k_i = \log K_i + \sum_{g=1}^{\bar{s}} n_g \log K_g \tag{6}$$

The K's are the equilibrium constants for the formation of the molecule from gaseous atoms (ref. 7).

The amount of heat transferred by conduction is given in terms of the flows and enthalpies of the molecular species by

$$W_f H_{f_o} - \sum_i^{\nu} W_i H_i = -4\pi r^2 \varkappa \frac{dT}{dr} \tag{7}$$

$H_{f_o}$ is the enthalpy of the fuel at its initial conditions and is a special case of $H_i$, the enthalpy of the $i^{th}$ species at temperature $T$; $H_i$ is $(H_T^o)_i$ of reference 7 and includes the chemical enthalpy.

And so for unknowns, there are $\nu + 1$ flows ($W_1$, $W_2$, . . . $W_i$, . . . $W_\nu$, $W_f$) and $\nu$ pressures ($p_1$, $p_2$, . . . $p_i$, . . . $p_\nu$). There are, therefore, $2\nu + 1$ unknowns in the system of equations. There are $s$ continuity equations (eqs. (1)), $\nu - 1$ diffusion equations (eqs. (2)), a total-pressure equation (eq. (3)), $\nu - s$ equilibrium equations (eqs. (5)), and an energy equation (eq. (7)) for a total of $2\nu + 1$ equations. At least in principle, the system of equations may be solved for all the $p_i$ and $W_i$ at any specified temperature.

The elimination of $W_f$ from the energy equation (7) and the continuity equations (1) yields a modified energy equation and $s - 1$ continuity equations. The diffusion equations are then used to eliminate the $W$'s from the energy and continuity equations. The symbol $\delta_i \equiv D_i/\varkappa RT$ (appendix E) is introduced for convenience throughout, and $dT/dr$ is introduced into the continuity equations. The results are an energy equation and continuity equations in terms of $\delta_i$, $H_i$, and $dp_i/dT$.

If the diffusion equations are taken in the form of equation (2a), the equations can be integrated numerically to produce a solution which is essentially exact (subject to the approximation in the transformation of appendix D). Some complications are encountered; an analytical solution of the equations is not possible. However, a numerical solution has been obtained for the carbon case; the significant equations and the difficulties are indicated in the next section.

If the diffusion expressions are taken in the form of equation (2b), the equations take the following form. The energy equation is

$$\sum_i \delta_i H_i \frac{dp_i}{dT} = -1 \tag{8}$$

and $\bar{s} - 1$ continuity equations

$$\sum_i c_i \delta_i \frac{dp_i}{dT} = 0 \tag{9}$$

In a specific case, $H_i'$ and $c_i$ develop in the algebra.

$H_i'$ and $\delta_i$ appearing in equations (8) and (9) are slowly varying functions of temperature over wide ranges of temperature. In addition, $\delta_i$ may vary with composition. For narrow temperature ranges, $\delta_i$ and $H_i'$ may be replaced by their mean values (in practice here, the $\delta_i$'s have been taken as constants). Then equations (8) and (9) may be integrated in closed form. 4076

The energy equation (eq. (8)) becomes

$$\Delta p_1 = \frac{\Delta T + \sum_{i \neq 1}^{\nu-1} \delta_i H_i' \Delta p_i}{-\delta_1 H_1'} \qquad i \neq N_2 \tag{10}$$

where $\Delta T = T - T_o$ and $\Delta p_i = p_{i,T} - p_{i,T_o}$.

The continuity equations (eqs. (9)) yield $\bar{s} - 1$ equations of the form

$$\Delta p_g = \frac{-1}{c_g \delta_g} \sum_{i \neq g}^{\nu-1} c_i \delta_i \Delta p_i \qquad i \neq N \quad \text{and} \quad g = 2, 3, \ldots \bar{s} \tag{11}$$

Further, there are $\nu - s$ equilibrium equations

$$p_i = k_i \prod_{g=1}^{\bar{s}} p_g^{-h_g} \tag{5}$$

and a total-pressure equation

$$p_{N_2} = P - \sum_{i \neq N_2}^{\nu} p_i \tag{3}$$

If minor inert gases are present, $p_{inert}$ = constant, and, therefore, $\Delta p_{inert} = 0$. The $p_1, p_2, \ldots, p_g, \ldots, p_{\bar{s}}$ on the left sides of equations (10) and (11) are the species previously selected as independent variables and which appear on the right side of equations (5).

Equations (10), (11), (5), and (3) in the forms indicated may be solved simultaneously. Values of $p_i$ at temperature $T$ $(p_{i,T})$ may be obtained provided that the values of $p_i$ at some nearby temperature $T_o$ $(p_{i,T_o})$ are available.

Knowing all the partial pressures $(p_{i,T_o})$ at some ambient boundary where $T = T_o$, select $T$ and guess first approximations for the $\bar{s}$ independent pressures. Using the equilibrium equations, compute first approximations for the remaining $p_{i,T}$ and then obtain second approximations for the independent variables using the integrated equations (10) and (11). Iterate to obtain constant values for all $p_{i,T}$ which now form a new set of boundary conditions. Select a new temperature and continue.

The iteration procedure is normally straightforward and convergent. While not always rapid, it can usually be accelerated by successive approximations based on the trend of the early steps. For several intervals in one system that converged in all other intervals, the iteration did diverge; in those intervals, successive approximations finally produced the answer.

The selection of temperature intervals is not critical. A major consideration should be the available tables of $K_i$ and $H_i$ (there is much less work if interpolation can be avoided). Generally, 400° K intervals proved satisfactory over most of the range, with 200° K intervals near the maximum temperature. It is probably desirable to have the upper limit of the highest temperature interval within 50° K of the maximum temperature. There is no particular reason for determining the maximum temperature.

At every temperature there are two sets of $p_i$ which satisfy the equations, one set corresponding to a fuel-lean condition and the other to a fuel-rich condition. Accidental interchange of these two conditions has not occurred; however, a very close approach to the maximum temperature might produce such confusion. On either side of the temperature maximum it is convenient to arrange equations (10), (11), and (5) so as to use as independent variables those species present in significant quantities in that region.

4076

CE-2

To end the calculation for either the numerical integration or the analytical solution, a boundary condition must be selected for the surface of the fuel particle; such a criterion may be either the surface temperature, the partial pressure of the fuel, or some equilibrium condition. The criteria for the work here are based on the latter two considerations. These critieria produced particle surface temperatures lower than those anticipated on the basis of the boiling point or the sublimation point. The effects of such differences on the burning rate are relatively small; however, it is felt that such criteria are more realistic than efforts to guess the probable surface temperature.

4076

Either the numerical integration or the use of equations (10) and (11) leads to a plot of partial pressure against temperature for each molecular species. Such plots are shown for carbon and boron in figure 2. The burning rate $W_f$ can be obtained from a suitable continuity equation; for example,

$$W_f = \frac{1}{k_f} \sum_i k_i W_{X_{k_i}} Y_{l_i} Z_{m_i} = \sum_i c_i' W_i \tag{12}$$

Substituting the appropriate diffusion equations (in this case, eq. (2b)) gives

$$-\frac{W_f}{4\pi r^2} = \varkappa \sum_i c_i' \delta_i \frac{dp_i}{dr} \tag{13}$$

Upon integration,

$$-W_f \int_{r_{T_o}}^{r_T} \frac{dr}{4\pi r^2} = \varkappa \sum_i c_i' \delta_i \int_{p_{i,T_o}}^{p_{i,T}} dp_i \tag{14}$$

for an interval corresponding to a temperature interval $\Delta T$ with limits $T_o$ and $T$, where the partial-pressure limits are $p_{i,T_o}$ and $p_{i,T}$ and the radius limits are $r_{T_o}$ and $r_T$. Then

$$\frac{W_f}{4\pi}\left(\frac{1}{r_T} - \frac{1}{r_{T_o}}\right) = \varkappa \sum_i c_i' \delta_i \Delta p_i \tag{15}$$

Summing $\Delta T$ from $T_C$ to $T_A$

$$\frac{W_f}{4\pi}\left(\frac{1}{r_A} - \frac{1}{r_C}\right) = \sum_{\Delta T}^{T_C \text{ to } T_A} \varkappa \sum_i c_i \delta_i \Delta p_i \tag{16}$$

corresponds to summing from the ambient boundary $r_C$ to the particle surface $r_A$. With $r_C \to \infty$, a value for $W_f/4\pi r_A$ is obtained. Summing in this way permits the use of an average value of $\varkappa$ for each temperature interval; as a first approximation, $\varkappa$ is the thermal conductivity of the inert (stagnant) gas from the ambient atmosphere.

The spatial structure of the flame is obtained from the ratio $\frac{W_f}{4\pi r}\Big/\frac{W_f}{4\pi r_A}$. Then

$$\frac{\frac{W_f}{4\pi r}}{\frac{W_f}{4\pi r_A}} = \frac{r_A}{r} = \frac{\sum_{\Delta T}^{T_C \text{ to } T} \varkappa \sum_i c_i \delta_i \Delta p_i}{\sum_{\Delta T}^{T_C \text{ to } T_A} \varkappa \sum_i c_i' \delta_i \Delta p_i} \tag{17}$$

where the denominator is the sum over all $\Delta T$, and the numerator is successive accumulated sums over $\Delta T$ intervals from the outer boundary to the value of the radius $r$. Flame structures so calculated are shown for carbon and boron in figure 3.

It should be noted that the geometry of the combustion system (spheres, cylinders, or plates) does not affect the partial-pressure - temperature curves involved in these calculations. Geometry is introduced only in finding the burning rate or the flame structure. Because of the mathematical forms of the various geometries, the spherical system is most convenient for theoretical treatments. In the spherical case, the ambient boundary appears as $1/r_C$, and the term approaches zero as the boundary is removed toward infinity; in the other cases, the ambient boundary appears explicitly in the final result. In a sense, the steady-state solution does not exist except for spheres.

## APPLICATION OF EQUATIONS

### Carbon

The combustion of a carbon particle in air is treated as a specific example of the general equations of the preceding section. The general

4076

CE-2 back

physical model is shown in figure 1(a), except that no assumptions are made about the structure. Carbon, oxygen, and nitrogen are $s = 3$ atom species. $C_1O_2N_0$, $C_1O_1N_0$, $C_0O_2N_0$, $C_0O_1N_0$, and $C_0O_0N_2$ are $\nu = 5$ molecular species, more familiarly, $CO_2$, CO, $O_2$, O, and $N_2$. The fuel is considered as $C_1O_0N_0$ and is not included as a molecular species because of the very low vapor pressure of carbon; this omission merely reduces the number of equilibrium equations by one. Then

$$\left.\begin{aligned} W_{carbon} &= W_{CO_2} + W_{CO} = 1W_f = W_f \\ W_{oxygen} &= 2W_{CO_2} + W_{CO} + 2W_{O_2} + W_O = 0W_f = 0 \\ W_{nitrogen} &= 2W_{N_2} = 0W_f = 0 \end{aligned}\right\} \tag{1$_C$}$$

4076

Numerical integration. - The diffusion equations for $\nu - 1 = 4$ species, $CO_2$, CO, $O_2$, and O, with the $\nu^{th}$ species identified as $N_2$, the only inert gas present, take the form

$$\frac{W_{CO_2}}{4\pi r^2} = \frac{-D_{CO_2}}{RT}\frac{dp_{CO_2}}{dr} - \frac{p_{CO_2}}{p_{N_2}}\left(\frac{D_{CO_2}}{RT}\frac{dp_{CO_2}}{dr} + \frac{D_{CO}}{RT}\frac{dp_{CO}}{dr} + \frac{D_{O_2}}{RT}\frac{dp_{O_2}}{dr} + \frac{D_O}{RT}\frac{dp_O}{dr}\right) \tag{2a$_C$}$$

and similarly for CO, $O_2$, and O. For $N_2$, the inert gas in the ambient atmosphere,

$$p_{N_2} = P - \sum_{i=1}^{4} p_i \tag{3$_C$}$$

The $\nu - s = 2$ equilibrium equations are written in terms of $\bar{s} = 2$ independent variables ($\bar{s} = s$ minus the number of inert species; $3 - 1 = 2$). $O_2$ and $CO_2$ have been selected as independent variables because these species predominate at the cold boundary. The chemical equations for CO are

4076

$$\left.\begin{aligned} CO_2 &= CO + \frac{1}{2} O_2 \\ CO + \frac{1}{2} O_2 - CO_2 &= 0 \text{ (zero)} \\ \text{and for O "molecules"} \\ O &= \frac{1}{2} O_2 \\ O - \frac{1}{2} O_2 &= 0 \text{ (zero)} \end{aligned}\right\} \tag{4$_C$}$$

The equilibrium equations are

$$\left.\begin{aligned} p_{CO} &= k_{CO} \frac{p_{CO_2}}{p_{O_2}^{1/2}} \\ p_O &= k_O p_{O_2}^{1/2} p_{CO_2}^{0} \end{aligned}\right\} \tag{5$_C$}$$

For example, in calculating $k_{CO}$ at 2000° K using values of $K_1$ from reference 7, equation (6) becomes

$$\left.\begin{aligned} \log k_{CO} &= \log K_{CO} + \frac{1}{2} \log K_{O_2} - \log K_{CO_2} \\ &= 21.1878 + \frac{1}{2} (6.2695) - 27.1855 = -2.8630 \\ k_{CO} &= 1.371 \times 10^{-3} \end{aligned}\right\} \tag{6$_C$}$$

The energy equation is

$$W_f H_{f_o} - W_{CO} H_{CO} - W_{CO_2} H_{CO_2} - W_{O_2} H_{O_2} - W_O H_O - W_{N_2} H_{N_2} = -4\pi r^2 \kappa \frac{dT}{dr} \tag{7$_C$}$$

With $W_f$ eliminated from equations (1$_C$) and (7$_C$), the energy equation becomes

$$W_{CO}(H_{CO} - H_{f_o}) + W_{CO_2}(H_{CO_2} - H_{f_o}) + W_{O_2} H_{O_2} + W_O H_O = 4\pi r^2 \kappa \frac{dT}{dr} \tag{7$_C$'}$$

Use the four diffusion equations ($2a_C$) to eliminate the four $W_i$'s, cancel $4\pi r^2$ and dr, introduce $\delta_i \equiv D_i/\kappa RT$, and rearrange. After considerable rearrangement, the energy equation becomes

$$(2 - p_{CO} - p_O)$$

$$\left[(H_{CO} - H_{f_o})\ \delta_{CO}\frac{dp_{CO}}{dT} + (H_{CO_2} - H_{f_o})\ \delta_{CO_2}\frac{dp_{CO_2}}{dT} + H_{O_2}\delta_{O_2}\frac{dp_{O_2}}{dT} + H_O\delta_O\frac{dp_O}{dT} + 1\right] +$$

$$\left[(H_{CO} - H_{f_o})\ p_{CO} + (H_{CO_2} - H_{f_o})\ p_{CO_2} + H_{O_2}p_{O_2} + H_O p_O\right]\left(\delta_{CO}\frac{dp_{CO}}{dT} + \delta_O\frac{dp_O}{dT}\right) = 0 \tag{8$_C$}$$

The continuity equation for oxygen can be similarly treated to yield

$$(2 - p_{CO} - p_O)\left(\delta_{CO_2}\frac{dp_{CO_2}}{dT} + \delta_{O_2}\frac{dp_{O_2}}{dT}\right) + (1 + p_{CO_2} + p_{O_2})\left(\delta_{CO}\frac{dp_{CO}}{dT} + \delta_O\frac{dp_O}{dT}\right) = 0 \tag{19$_C$}$$

The equilibrium equations are

$$\left.\begin{aligned} p_O &= k_O p_{O_2}^{1/2} \\ p_{CO} &= k_{CO}\frac{p_{CO_2}}{p_{O_2}^{1/2}} \end{aligned}\right\} \tag{5$_C$}$$

Further, the derivatives of the equilibrium equations are required for the numerical integration

$$\left.\begin{aligned} \frac{dp_O}{dT} &= k_O p_{O_2}^{1/2}\left(\frac{H_O - \frac{1}{2}H_{O_2}}{RT^2} + \frac{1}{2p_{O_2}}\frac{dp_{O_2}}{dT}\right) \\ \text{and} \quad \frac{dp_{CO}}{dT} &= k_{CO}\frac{p_{CO_2}}{p_{O_2}^{1/2}}\left(\frac{H_{CO} + \frac{1}{2}H_{O_2} - H_{CO_2}}{RT^2} + \frac{1}{p_{CO_2}}\frac{dp_{CO_2}}{dT} - \frac{1}{2p_{O_2}}\frac{dp_{O_2}}{dT}\right) \end{aligned}\right\} \tag{20$_C$}$$

4076

The energy equation (eq. ($18_C$)), the continuity equation (eq. ($19_C$)), the equilibrium equations (eqs. ($5_C$)), and the derivatives of the equilibrium equations (eqs. ($20_C$)), in the forms indicated, may be integrated numerically using the second method of reference 8. This has been done using for the cold-boundary conditions (at C): $T = 300^\circ$ K, $p_{O_2} = 0.2095$, $p_{CO_2} = p_{CO} = p_O = 0$. The quantity $\delta_i$ (appendix E) was assumed to be independent of temperature and composition. Values of $K_i$ for equation ($6_C$) and $H_i$ were obtained from reference 7.

4076

In the numerical integration, the temperature is a very satisfactory running variable, because $H_i$ and $K_i$ are tabulated at 100° C intervals. However, at the maximum temperature all $dp_i/dT = \infty$. Therefore, the running variable must be changed at some suitably high temperature (in this case a shift from $T$ to $p_{CO}$ was made, which yielded $dp_i/dp_{CO}$ and $dT/dp_{CO}$).

The boundary condition for ending the calculation of the temperature-composition profile was selected as the temperature at which $p_{CO}$ and $p_{CO_2}$ satisfy the equilibrium for the reaction

$$\left.\begin{aligned} C + CO_2 &= 2CO \\ k_C &= \frac{p_{CO}^2}{p_{CO_2}} \end{aligned}\right\} \qquad (21_C)$$

This boundary condition corresponds closely to $p_{CO_2} = 0$. The results of the numerical integration are values of $p_{CO}$, $p_{CO_2}$, $p_O$, and $p_{O_2}$ at various temperatures (fig. 2(a)); $p_{N_2}$ follows directly from equation ($3_C$).

The burning rate is obtained by substituting the diffusion equations into the continuity equation for carbon (the procedure is analogous to that yielding equations (12) to (16)):

$$\frac{W_f}{4\pi r^2}\,dr =$$

$$-\varkappa\left[\delta_{CO}dp_{CO} + \delta_{CO_2}dp_{CO_2} + \frac{p_{CO_2} + p_{CO}}{p_{N_2}}\left(\delta_{CO}dp_{CO} + \delta_{CO_2}dp_{CO_2} + \delta_{O_2}dp_{O_2} + \delta_O dp_O\right)\right] \qquad (22_C)$$

Upon integration, each set of $\Delta p_i$ corresponding to a particular $\Delta T$ corresponds to an increment in space. The sum over all $\Delta T$ intervals from $T_C$ to $T_A$ when $r_C = \infty$ and $r_A$ equals the particle radius yields the burning rate $W_f$:

$$\frac{W_f}{4\pi r_A} = \sum_{\Delta T}^{T_C \text{ to } T_A} \left[\varkappa(\delta_{CO}\Delta p_{CO}+\delta_{CO_2}\Delta p_{CO_2})+\varkappa\left(\frac{p_{CO_2}+p_{CO}}{p_{N_2}}\right)(\delta_{CO}\Delta p_{CO}+\delta_{CO_2}\Delta p_{CO_2}+\delta_{O_2}\Delta p_{O_2}+\delta_O\Delta p_O)\right] \tag{23$_C$}$$

where $\varkappa$ and the factor $\varkappa \frac{p_{CO_2} + p_{CO}}{p_{N_2}}$ are taken as average values over the temperature interval corresponding to $\Delta p_i$. The burning rate is reported in the RESULTS section.

The complete structure for the carbon particle diffusion flame (fig. 3(a)) is traced out in terms of equation ($23_C$) as described in connection with equation (17).

Analytical solution. - To carry out the analytical solution instead of the numerical integration, the diffusion equations are taken in the form

$$\frac{W_i}{4\pi r^2} = -\frac{D_i}{RT}\frac{dp_i}{dr} \tag{2b$_C$}$$

The energy and continuity equations appear in the form indicated by equations (8) and (9). The appropriate equations can be derived by the steps indicated or can be obtained by setting all $p_i$ (but not $dp_i/dT$ or $\Delta p_i$) equal to zero in equations ($18_C$), ($19_C$), ($22_C$), and ($23_C$). The energy equation is

$$\delta_{CO}(H_{CO} - H_{f_o})\frac{dp_{CO}}{dT} + \delta_{CO_2}(H_{CO_2} - H_{f_o})\frac{dp_{CO_2}}{dT} + \delta_{O_2}H_{O_2}\frac{dp_{O_2}}{dT} + \delta_O H_O\frac{dp_O}{dT} = -1 \tag{8$_C$}$$

The oxygen continuity equation is

$$2\delta_{CO_2}\frac{dp_{CO_2}}{dT} + 2\delta_{O_2}\frac{dp_{O_2}}{dT} + \delta_{CO}\frac{dp_{CO}}{dT} + \delta_{O}\frac{dp_{O}}{dT} = 0 \tag{9$_C$}$$

The equations may be integrated at once, provided a small enough interval is selected so that the enthalpy terms and $\delta_i$ may be approximated by average values. On the oxygen-rich side, $p_{O_2}$ and $p_{CO_2}$ are appreciable and are selected as independent variables. The elimination of $\delta_{O_2}\frac{dp_{O_2}}{dT}$ from the energy equation results in a slight additional simplification. Then

$$\Delta p_{CO_2} = \frac{\Delta T + \delta_{CO}H'_{CO}\Delta p_{CO} + \delta_{O}H'_{O}\Delta p_{O}}{-\delta_{CO_2}H'_{CO_2}} \tag{10$_C$}$$

and

$$\Delta p_{O_2} = -\frac{1}{\delta_{O_2}}\left(\frac{\delta_{CO}}{2}\Delta p_{CO} + \frac{\delta_{O}}{2}\Delta p_{O} + \delta_{CO_2}\Delta p_{CO_2}\right) \tag{11$_C$}$$

where

$$H'_{CO} = H_{CO} - H_{f_o} - \frac{H_{O_2}}{2}$$

$$H'_{O} = H_{O} - \frac{H_{O_2}}{2}$$

$$H'_{CO_2} = H_{CO_2} - H_{f_o} - H_{O_2}$$

Equations ($10_C$) and ($11_C$) are iterated together with the equilibrium equations (eqs. ($5_C$)) from the outer boundary toward the region of maximum temperature, that is, over the oxygen-rich side of the flame front.

On the fuel-rich side, $p_{CO_2}$ and $p_{CO}$ are the major constituents and are selected as the independent variables. Eliminate $\delta_{CO} \frac{dp_{CO}}{dT}$ from the energy equation. Then

$$\Delta p_{CO_2} = \frac{\Delta T + \delta_{O_2} H''_{O_2} \Delta p_{O_2} + \delta_O H''_O \Delta p_O}{- \delta_{CO_2} H''_{CO_2}} \tag{10$_C$'}$$

4076

and

$$\Delta p_{CO} = - \frac{1}{\delta_{CO}} \left(\delta_O \Delta p_O + 2\delta_{O_2} \Delta p_{O_2} + 2\delta_{CO_2} \Delta p_{CO_2}\right) \tag{11$_C$'}$$

where

$$H''_O = H_O - H_{CO} + H_{f_o}$$

$$H''_{O_2} = H_{O_2} - 2H_{CO} + 2H_{f_o}$$

$$H''_{CO} = H_{CO_2} + H_{f_o} - 2H_{CO}$$

The equilibrium equations (eqs. ($5_C$)) must also be rearranged in terms of $p_{CO_2}$ and $p_{CO}$

$$\left.\begin{array}{ll} O_2 - 2CO_2 + 2CO = 0 \text{ (zero)} & O + CO - CO_2 = 0 \text{ (zero)} \\ p_{O_2} = \left(k_{CO} \dfrac{p_{CO_2}}{p_{CO}}\right)^2 & p_O = k_O k_{CO} \dfrac{p_{CO_2}}{p_{CO}} \end{array}\right\} \tag{5$_C$'}$$

$k_{CO}^2$ and $k_O k_{CO}$ may be used as determined before but are better evaluated directly in terms of the $K_1$ to avoid a buildup in rounding-off errors. This system of equations (eqs. ($5_C$'), ($10_C$'), and ($11_C$')) may be iterated just as on the oxygen-rich side of the maximum temperature.

The shift from one set of equations to the other is best made after approaching to within 50° K of the maximum temperature. Using the last set of $p_i$ and T found on the oxygen-rich side, guesses are made for

$p_{CO}$ and $p_{CO_2}$ at the same $T$ on the fuel-rich side. The iteration procedure is similar, except that with $\Delta T = 0$ it is more sensitive to small changes in $\Delta p_i$.

The burning rate is given as

$$\frac{W_f}{4\pi r_A} = \sum_{\Delta T}^{T_C \text{ to } T_A} \varkappa(\delta_{CO}\Delta p_{CO} + \delta_{CO_2}\Delta p_{CO_2}) \tag{16$_C$}$$

and the structure of the flame is as in equation (17). The equations can be obtained from equations ($22_C$) and ($23_C$) by setting $p_i = 0$ (but not $\Delta p_i$), except for $i = N_2$. The burning rate is reported in the RESULTS section. The structure is plotted in figure 3(a).

## Boron

The burning rate of a boron particle is treated in appendix B by the methods outlined in the section GENERAL EQUATIONS. Because so many equilibrium equations exist, the numerical integration is not carried out; rather, the analytical solution using the iterative procedure is applied to four separate boundary conditions. The derivation of a boundary condition for condensed $B_2O_3$ is included in appendix B. Also included are the details of a rapid three-graph method for obtaining the burning rate of boron under a variety of ambient conditions; this graphical method is of general use in cases in which some medium temperature boundary exists.

Figure 2(b) shows curves of partial pressure against temperature for boron burning in air; figure 3(b) gives the flame structure for the same case. The burning rates from the analytical solution and from the simplified equations (appendix C) are presented in the RESULTS section and in tables I and II.

## Hydrocarbons

Simplified calculations of burning rate have been made previously for hydrocarbons in terms of heat conduction and diffusion. References 1 and 5 give results of calculations showing the effect on burning rate of certain changes in the basic assumptions involved. The equations used in those calculations can be deduced from the general equations presented in earlier sections of this report by introducing certain assumptions about boundary conditions inside the flame.

4076

CH-3 back

The details of the reduction of the general equations to the simplified equations previously used are contained in appendix C. The use of the simplified equations leads to an expression for $W_f/4\pi r_A$ for the burning rate, as does use of the extended calculation. The only information which can be deduced about the structure of the flame is the location of the flame front.

The burning rate of isooctane (a typical hydrocarbon) in air is included in the RESULTS section. Values for other ambient oxygen partial pressures and temperatures may be readily obtained from reference 5 as indicated in appendix C.

4076

## Magnesium

Work has been published on the experimental burning times (inverse rates) of magnesium ribbons in various atmospheres (ref. 6). The calculations presented with that work support the experimental results quite closely in the prediction of relative rates; however, the calculations were based on equations deduced from the equations used for hydrocarbons (refs. 1 and 5) rather than from the general equations like those presented here. If the equations for the magnesium case are deduced from the equations in the GENERAL EQUATIONS section, the resulting equations have a somewhat different form than those appearing in reference 6. These changes have some effects on the results of the previous calculations for magnesium. The computed burning rates decrease somewhat (burning times increase); the predicted relative rates are somewhat less strongly dependent upon the ambient oxygen partial pressure.

The details of the reduction of the general equations are contained in appendix C. The burning rate is obtained as $W_f/4\pi r_A$. The only information obtained about the flame structure is the location of the inner and outer boundaries of the high-temperature zone.

## RESULTS

When the calculations described in the GENERAL EQUATIONS section are applied to carbon as a specific example, and to boron (appendix B), they yield the burning rate and the flame structure of the diffusion flame; these come as simple consequences of temperature-composition curves which are the direct result of the numerical integration or the iteration of the analytical solution. Temperature-composition curves are shown in figure 2(a) for carbon and in figure 2(b) for boron. The flame structure of carbon is indicated in figure 3(a) and of boron in figure 3(b). Burning rates are presented in table I.

For carbon, figures 2(a) and 3(a) give the results of both the numerical integration and the iterative procedure. They do not differ significantly. In the oxygen-rich region below 2100° K, where the diffusion of $O_2$ and $CO_2$ is actually equimolar counterdiffusion, the numerical integration and the analytical solution (based on diffusion equations (2b) of the same form as those for equimolar counterdiffusion) give identical plots of partial pressures against temperature. In the fuel-rich region, the partial-pressure - temperature curves diverge for the two cases; two molecules of CO pass out for each molecule of $CO_2$ going in. The burning rates for the two carbon calculations agree well. This is an indication that the considerably less difficult analytical solution does not introduce significant variations in the results.

4076

Figures 2(b) and 3(b) show the partial-pressure - temperature curve and the flame structure for boron burning in air from the analytical solution (appendix B). For boron, the analytical solution involving the iterative procedure is applied to four separate boundary conditions. These results (fig. 4), together with two curves (figs. 5 and 6) representing boundary conditions for the condensed oxide, yield boron burning rates for a wide variety of ambient temperature and oxygen concentration.

The following paragraph is an example of the use of figures 4 to 6 - finding the burning rate of boron $W_f/4\pi r_A$ for an ambient temperature of 400° K in a mixture of 18 percent $O_2$ and 82 percent $N_2$ by volume at 1 atmosphere. From figure 5, the correction term $\Delta p_{O_2} = 0.0514$; then $p_{O_2 1570} = 0.1800 - 0.0514 = 0.1286$. From figure 6, for 400° K, $(W_f/4\pi)(1/r_{1570} - 1/r_C) = 1.21\times10^{-6}$ mole per centimeter per second; from figure 4, for $p_{O_2 1570} = 0.1286$ atm, $(W_f/4\pi)(1/r_A - 1/r_{1570}) = 8.33\times10^{-6}$ mole per centimeter per second. Therefore, with $1/r_C = 0$, $W_f/4\pi r_A = 9.54\times10^{-6}$ mole per centimeter per second.

The simplified equations deduced in appendix C from the general equations are applied to boron. The calculations were carried out for two extremely different composition conditions (case A, solely oxygen and product, case B, product and nitrogen); note remarks on the treatment of dissociation in appendix C. The values of $W_f/4\pi r_A$ obtained (table I) are in substantial agreement, although the values of $T_B$ varied widely. The only significant difference in the two cases arises when ambient temperature and oxygen partial pressure are varied (table II).

The burning rates for boron obtained from the extended calculations are shown in table II. For a series of increasing ambient temperature, the burning rate in air increases roughly 1 to 2 percent per 100° K;

reducing the initial oxygen partial pressure from 0.21 to 0.15 atmosphere at 800° K decreases the burning rate by roughly one-third. Case A of the simplified calculation gives numerical answers rather close to those of the extended calculation, but there is little variation with ambient temperatures and oxygen partial pressure. Case B of the simplified equations gives numbers about 50 percent greater than those of the extended calculation; however, the relative dependence of the burning rate upon ambient temperature and oxygen partial pressure is similar for case B and the extended calculation. When the results of the extended calculations are compared with those of the simplified equations, it appears that for many purposes the simplified calculations should prove adequate.

The numerical results of the calculations described yield burning rates which may be expressed in a variety of ways. For the spherical geometry considered here, this leads to values of $W_f/4\pi r_A$ which include the steady-state assumption that $1/r_C$ has gone to zero. The units of the integrals are (moles of fuel)/(cm)(sec). These results are converted to the more physically significant units of fuel consumption, g/(cm)(sec), or heat-release rate, cal/(cm)(sec), by introducing the molecular weight of the fuel or its molar heat of combustion. Table I gives values of $W_f/4\pi r_A$ in a variety of units for carbon, boron, isooctane, and magnesium.

The evaporation constant and particle lifetimes for 1-micron particles are also included in table I. These values are based on the assumption that these particles obey the formula for evaporation, which includes burning as a special case (refs. 2 and 5),

$$d^2 = d_o^2 - \beta' t$$

where $d_o$ is the drop diameter at $t = 0$, $d$ is the diameter at $t$, and $\beta'$ is the evaporation constant. The droplet lifetime is then

$$t_l = \frac{d_o^2}{\beta'}$$

where $\beta' = 8\times10^8 \frac{M}{\rho} \frac{W_f}{4\pi r_A}$ square microns per second.

On a weight and heat-release basis (table I) isooctane and magnesium have rates which are roughly three to five times greater than those of boron and carbon. (Molar rates are not a meaningful comparison for substances of different molecular weight.) In terms of particle lifetimes, those of boron and carbon are an order of magnitude greater than those of isooctane and magnesium.

The burning-rate calculations (which apply only to steady-state burning) do not in themselves explain the extreme difficulty of burning elemental boron (e.g., incomplete combustion even in a bomb calorimeter (ref. 9)). The computed structure does indicate large concentrations of gaseous boric oxide ($B_2O_3$) near the boron surface. During ignition or under convective conditions, a momentarily cool boron surface might become coated with condensed oxide; such a coating could well preclude complete combustion.

4076

## SUMMARY OF RESULTS

A system with general equations for computing the burning rates of small particles has been developed and applied to the combustion of carbon, boron, magnesium, and isooctane, with the following results:

1. Burning rates of liquid hydrocarbons and relative rates for magnesium ribbons have been predicted in satisfactory agreement with experiment from a model in which heat- and mass-transfer processes are assumed rate determining.

2. The equations which determine the steady-state burning of liquids or solids can be set down in a general form. From these general equations, together with appropriate simplifying assumptions, the explicit burning-rate equations which have been used previously for hydrocarbons and magnesium may be derived.

3. If dissociation is considered in the calculations, more realistic temperature and composition profiles are obtained for the combustion zone. However, such considerations do not change burning rates greatly from those calculated from highly simplified models.

4. Calculations indicate that heat-release rates are in the order: liquid hydrocarbons > magnesium > boron ≅ carbon.

5. The burning-rate calculations (which apply only to steady-state burning) do not in themselves explain the extreme difficulty of burning elemental boron.

Lewis Flight Propulsion Laboratory
National Advisory Committee for Aeronautics
Cleveland, Ohio, December 14, 1956

# APPENDIX A

## SYMBOLS

The following symbols are used in this report (the units indicated are those employed here, but the equations are valid for any consistent set of units):

| | |
|---|---|
| $\underline{B}$,$\underline{B}'$,$\underline{C}$ | definite integrals defined in text, moles/(cm)(sec) |
| C | differential function defined by equation (D3) |
| c,c' | constants, developed explicitly in any specific example |
| D | diffusion coefficient, sq cm/sec |
| d | diameter, microns |
| F(T) | right side of equation ($32_B$) |
| G | mass-transfer rate per unit area, moles/(sq cm)(sec) |
| g | general independent molecular species |
| H | enthalpy, including chemical energy, cal/mole |
| $\Delta H$ | sensible heat of fuel to boiling point, cal/mole |
| H',H" | sums of enthalpies, developed explicity in any specific example, cal/mole |
| $\mathscr{H}$ | heat of combustion/heat of vaporization |
| K | equilibrium constant for reference reactions |
| k | equilibrium constant for specified reaction |
| L | heat of vaporization, cal/mole |
| M | molecular weight, g/mole |
| n | stoichiometric coefficient |
| P | total pressure, atm |
| p | partial pressure, atm |
| Q | heat of combustion at reference temperature, cal/mole |

4076

4076

CE-4

| | |
|---|---|
| $R$ | universal gas constant $\begin{cases} 82.05 \text{ (cu cm)(atm)/(}^{\circ}\text{C)(mole)} \\ 1.987 \text{ cal/(}^{\circ}\text{C)(mole)} \end{cases}$ |
| $r$ | radius from center of particle, cm |
| $s$ | number of atom species |
| $\bar{s}$ | $s$ minus the number of inert species; number of molecular species adopted as independent variables |
| $T$ | absolute temperature, $^{\circ}$K |
| $t$ | time, sec |
| $t_l$ | lifetime of particle, sec |
| $\bar{V}$ | diffusion velocity, cm/sec |
| $W$ | mass-transfer rate, moles/sec |
| $X,Y,Z$ | atom species |
| $X_{k_i}Y_{l_i}Z_{m_i}$ | general molecular species |
| $x$ | mole fraction, $p/P$ |
| $\beta_{ij}$ | $D_{ij}$ $P/RT$, mole/(cm)(sec) |
| $\beta'$ | evaporation constant, sq microns/sec |
| $\delta$ | $D/\varkappa RT$, (moles)($^{\circ}$C)/(cal)(atm) |
| $\varkappa$ | thermal conductivity, cal/(sq cm)(sec)($^{\circ}$C/cm) |
| $\nu$ | number of molecular species |
| $\rho$ | fuel density, g/cc |
| $\sigma$ | molecular diameter, Angstroms |
| $\Omega(1,1)^*$, $\Omega(2,2)^*$ | integrals for calculation of diffusion coefficient and thermal conductivity, tabulated in ref. 10 |

Subscripts:

| | |
|---|---|
| A,B,B',C | boundaries of zones (fig. 1) |

| | |
|---|---|
| AB,BB',BC,B'C | zones between appropriate boundaries |
| (c) | condensed phase |
| eq | equilibrium |
| f | fuel |
| (g) | gaseous phase |
| i,j | general molecular species |
| o | initial conditions |
| p | combustion products |

4076

# APPENDIX B

## DETAILS OF BORON TREATMENT

This appendix presents the details of the treatment of boron in terms of the general equations. This includes the equations for the analytical solution, as well as the derivation of a boundary condition for condensed $B_2O_3$. Further, there is an explanation of the rapid three-graph method for obtaining burning rates of boron under a variety of ambient conditions; an example appears in the RESULTS section.

4076

### General Boron System with Gaseous $B_2O_3$

The general physical model is that indicated in figure 1(a), except that no assumptions are made about the structure of the flame. Heat and mass transfer are considered; convection is assumed to be absent. As distinct from carbon, boron is significantly volatile at flame temperature. Nevertheless, the handling of the equations is quite analagous to the carbon case.

CE-4, back

Boron, oxygen, and nitrogen are $s = 3$ atom species corresponding to X, Y, Z of the general treatment. B, $B_2$, BO, $B_2O_3$, O, $O_2$, and $N_2$ are $\nu = 7$ molecular species corresponding to $B_1O_0N_0$, $B_2O_0N_0$, $B_1O_1N_0$, $B_2O_3N_0$, $B_0O_1N_0$, $B_0O_2N_0$, and $B_0O_0N_2$ in the notation of the general case. $B_1O_0N_0$ is assumed to be the fuel molecule.

The continuity equations are

$$\left.\begin{aligned} W_{Boron} &= W_B + 2W_{B_2} + W_{BO} + 2W_{B_2O_3} = 1W_f = W_f \\ W_{Oxygen} &= W_{BO} + 3W_{B_2O_3} + W_O + 2W_{O_2} = 0W_f = 0 \\ W_{Nitrogen} &= 2W_{N_2} = 0W_f = 0 \end{aligned}\right\} \qquad (1_B)$$

From the diffusion equation (eq. (2b)), the $\nu - 1 = 6$ diffusion equations are of the form

$$\frac{W_B}{4\pi r^2} = -\frac{D_B}{RT}\frac{dp_B}{dr} \qquad (2b_B)$$

and similarly for $B_2$, BO, $B_2O_3$, O, and $O_2$.

The total-pressure equation for nitrogen is

$$p_{N_2} = P - \sum_{i \neq N_2} p_i \tag{$3_B$}$$

For independent variables, $\bar{s} = 2$ ($s = 3$ minus 1 inert species, $N_2$); $O_2$ and $B_2O_3$ are the noninert species with greatest partial pressures near the cold boundary. The $\nu - s = 4$ chemical and equilibrium equations are 4076

$$\left.\begin{aligned}
&\tfrac{1}{2} B_2O_3 = B + \tfrac{3}{4} O_2 \\
&B + \tfrac{3}{4} O_2 - \tfrac{1}{2} B_2O_3 = 0 \text{ (zero)} \\
&B_2O_3 = B_2 + \tfrac{3}{2} O_2 \\
&B_2 + \tfrac{3}{2} O_2 - B_2O_3 = 0 \text{ (zero)} \\
&\tfrac{1}{2} B_2O_3 = BO + \tfrac{1}{4} O_2 \\
&BO + \tfrac{1}{4} O_2 - \tfrac{1}{2} B_2O_3 = 0 \text{ (zero)} \\
&\tfrac{1}{2} O_2 = O \\
&O - \tfrac{1}{2} O_2 = 0 \text{ (zero)}
\end{aligned}\right\} (4_B) \qquad \left.\begin{aligned}
&p_B = k_B \frac{p_{B_2O_3}^{1/2}}{p_{O_2}^{3/4}} \\
&p_{B_2} = k_{B_2} \frac{p_{B_2O_3}}{p_{O_2}^{3/2}} \\
&p_{BO} = k_{BO} \frac{p_{B_2O_3}^{1/2}}{p_{O_2}^{1/4}} \\
&p_O = k_O p_{O_2}^{1/2}
\end{aligned}\right\} (5_B)$$

The energy equation takes the form

$$W_f H_{f_o} - W_B H_B - W_{B_2} H_{B_2} - W_{BO} H_{BO} - W_{B_2O_3} H_{B_2O_3} - W_O H_O - W_{O_2} H_{O_2} = -4\pi r^2 \times \frac{dT}{dr} \tag{$7_B$}$$

As in the general equations, the energy equation and the oxygen continuity equation can be transposed to give

$$\delta_B(H_B - H_{f_o}) \frac{dp_B}{dT} + \delta_{B_2}(H_B - 2H_{f_o}) \frac{dp_B}{dT} + \delta_{BO}(H_{BO} - H_{f_o}) \frac{dp_{BO}}{dT} +$$

$$\delta_{B_2O_3}(H_{B_2O_3} - 2H_{f_o}) \frac{dp_{B_2O_3}}{dT} + \delta_O H_O \frac{dp_O}{dT} + \delta_{O_2} H_{O_2} \frac{dp_{O_2}}{dT} = -1 \qquad (8_B)$$

4076

and

$$\delta_{BO} \frac{dp_{BO}}{dT} + 3\delta_{B_2O_3} \frac{dp_{B_2O_3}}{dT} + \delta_O \frac{dp_O}{dT} + 2\delta_{O_2} \frac{dp_{O_2}}{dT} = 0 \qquad (9_B)$$

Equations $(8_B)$ and $(9_B)$ may be integrated using mean values of $\delta_i$ and $H_i$, and each equation solved for one of the two independent variables.

As in the carbon case, it is convenient to eliminate the second independent variable from the energy equation; $\delta_{B_2O_3} \frac{dp_{B_2O_3}}{dT}$ is eliminated. Independent variables are $p_{B_2O_3}$ and $p_{O_2}$ on the oxygen-rich side, $p_{B_2O_3}$ and $p_{BO}$ on the fuel-rich side.

The energy equation (on the oxygen-rich side) is

$$\Delta p_{O_2} = \frac{\Delta T + \delta_B H_B' \Delta p_B + \delta_{B_2} H_{B_2}' \Delta p_{B_2} + \delta_{BO} H_{BO}' \Delta p_{BO} + \delta_O H_O' \Delta p_O}{-\delta_{O_2} H_{O_2}'} \qquad (10_B)$$

The continuity equation is

$$\Delta p_{B_2O_3} = \frac{-1}{3\delta_{B_2O_3}} (\delta_{BO} \Delta p_{BO} + \delta_O \Delta p_O + 2\delta_{O_2} \Delta p_{O_2}) \qquad (11_B)$$

Equations $(10_B)$ and $(11_B)$ together with the equilibrium equations (eqs. $(5_B)$) and the total-pressure equation (eq. $(3_B)$) for nitrogen may be iterated, as in the general case and the carbon example, as soon as cold boundary conditions are available; however, such a solution is possible only when the system is entirely gaseous.

## Condensed $B_2O_3$, a Special Boundary Condition

When condensed $B_2O_3$ is present, temperature is relatively low; B, $B_2$, BO, and O are essentially absent; and $N_2$, $O_2$, $B_2O_3(g)$, and $B_2O_3(c)$

are present. The symbols (g) and (c) with $B_2O_3$ stand for gaseous and condensed (liquid or solid) oxide, respectively. For these conditions, the continuity equations assume the form

$$\left.\begin{aligned} 2W_{B_2O_3(g)} + 2W_{B_2O_3(c)} &= W_f \\ 3W_{B_2O_3(g)} + 3W_{B_2O_3(c)} + 2W_{O_2} &= 0 \\ W_{N_2} &= 0 \end{aligned}\right\} \tag{24$_B$}$$

4076

The diffusion equations for $B_2O_3(g)$ and $O_2$ are

$$\left.\begin{aligned} \frac{W_{B_2O_3(g)}}{4\pi r^2} &= -\frac{D_{B_2O_3}}{RT}\frac{dp_{B_2O_3}}{dr} \\ \frac{W_{O_2}}{4\pi r^2} &= -\frac{D_{O_2}}{RT}\frac{dp_{O_2}}{dr} \end{aligned}\right\} \tag{25$_B$}$$

For nitrogen

$$p_{N_2} = P - p_{O_2} - p_{B_2O_3(g)} \tag{26$_B$}$$

The equilibrium partial pressure of $B_2O_3$ is given by

$$\log p_{eq,B_2O_3} = \log K_{B_2O_3(g)} - \log K_{B_2O_3(c)} \tag{27$_B$}$$

The energy equation is

$$W_f H_{f_o} - W_{B_2O_3(g)}H_{B_2O_3(g)} - W_{B_2O_3(c)}H_{B_2O_3(c)} - W_{O_2}H_{O_2} - W_{N_2}H_{N_2} = -4\pi r^2 \varkappa \frac{dT}{dr} \tag{28$_B$}$$

Combining equations (24$_B$), (25$_B$), and (28$_B$) yields

$$\delta_{B_2O_3}\left(H_{B_2O_3(g)} - H_{B_2O_3(c)}\right)\frac{dp_{B_2O_3(g)}}{dT} + \delta_{O_2}\left[H_{O_2} - \frac{2}{3}\left(H_{B_2O_3(c)} - 2H_{f_o}\right)\right]\frac{dp_{O_2}}{dT} = -1 \tag{29$_B$}$$

Since $p_{B_2O_3(g)} = p_{eq,B_2O_3}$,

$$\frac{dp_{B_2O_3(g)}}{dT} = \frac{dp_{eq,B_2O_3}}{dT} = p_{eq,B_2O_3} \frac{H_{B_2O_3(g)} - H_{B_2O_3(c)}}{RT^2} \tag{30$_B$}$$

Substituting for $dp_{B_2O_3}/dT$ in equation ($29_B$) gives the following expression for $dp_{O_2}/dT$:

$$-\frac{dp_{O_2}}{dT} =$$

$$\frac{1}{\delta_{O_2}\left[H_{O_2} - \frac{2}{3}\left(H_{B_2O_3(c)} - 2H_{f_o}\right)\right]}\left[1 + \frac{p_{eq,B_2O_3}\delta_{B_2O_3}\left(H_{B_2O_3(g)} - H_{B_2O_3(c)}\right)^2}{RT^2}\right] \tag{31$_B$}$$

A second expression for $dp_{O_2}/dT$ is obtained by setting $W_{B_2O_3(c)} = 0$ in the oxygen continuity equation for the boundary at which the condensed oxide vanishes, then substituting the diffusion equations for $W_{B_2O_3(g)}$ and $W_{O_2}$:

$$-\frac{dp_{O_2}}{dT} = \frac{3}{2}\frac{\delta_{B_2O_3}}{\delta_{O_2}}\frac{dp_{B_2O_3}}{dT} = \frac{3}{2}\frac{\delta_{B_2O_3}}{\delta_{O_2}}\frac{p_{eq,B_2O_3}\left(H_{B_2O_3(g)} - H_{B_2O_3(c)}\right)}{RT^2} \tag{32$_B$}$$

A graphical solution of these two expressions for $dp_{O_2}/dT$ in terms of $p_{eq,B_2O_3}$ indicates that the two functions are equal at a temperature of 1570° K, which corresponds to $p_{B_2O_3} = 0.004365$ atmosphere. This is essentially a dew point for $B_2O_3$ in the combustion system; it is independent of the ambient temperature and the ambient partial pressure of oxygen, but would be affected by any variation of $H_{f_o}$, $\delta_{O_2}$, or $\delta_{B_2O_3}$. The condition $W_{B_2O_3(c)} = 0$ as a condition at the dew point is somewhat arbitrary; however, no diffusion equation can be written for the condensed phase, and there is no basis for assigning a flow velocity other than zero to condensing particles of $B_2O_3$. The condensed $B_2O_3$ particles are implicitly assumed to move, in other regions, at the velocity necessary to maintain the steady state.

The partial pressure of oxygen corresponding to $T = 1570^\circ$ K and $p_{B_2O_3,1570}$ is obtained by integrating equation $(31_B)$ graphically to yield $p_{O_2,1570}$:

$$\int_{T_C}^{1570} F(T)\ dT = -\Delta p_{O_2} = p_{O_2C} - p_{O_2 1570} \tag{$33_B$}$$

where $F(T)$ is the right side of equation $(31_B)$. Figure 5 is a plot of the integral as a function of $T_C$ (the value of $\Delta p_{O_2}$ is a correction to the ambient partial pressure of oxygen $(p_{O_2C})$ for the departure of the ambient temperature from $1570^\circ$ K). 4076

## Burning Rate and Flame Structure

In the regions where condensed $B_2O_3$ exists, the continuity equations $(24_B)$ can be combined with the diffusion equation for oxygen (eq. $(25_B)$). This yields

$$W_f = -\frac{4}{3} W_{O_2} = \frac{4}{3} \varkappa \delta_{O_2}\ 4\pi r^2 \frac{dp_{O_2}}{dr} \tag{$34_B$}$$

which when integrated from the ambient boundary ($T_C$, $p_{O_2C}$, and $r_C$) to the boundary conditions ($1570^\circ$ K, $p_{O_2 1570}$, and $r_{1570}$) gives by equation $(33_B)$

$$\left.\begin{aligned} \frac{W_f}{4\pi}\left(\frac{1}{r_{1570}} - \frac{1}{r_C}\right) &= -\frac{4}{3} \varkappa \delta_{O_2}(p_{O_2 1570} - p_{O_2C}) \\ &= \frac{4}{3} \delta_{O_2} \int_{T_C}^{1570} \varkappa F(T)\ dT \end{aligned}\right\} \tag{$35_B$}$$

Figure 6 is a plot of the integral as a function of $T_C$ calculated assuming $\varkappa = \varkappa_{N_2}$. The value of the integral in equation $(35_B)$ would yield the burning rate if $r_{1570}$ could be determined; as it stands the integral is a quantity which may be added to the quantity $\frac{W_f}{4\pi}\left(\frac{1}{r_A} - \frac{1}{r_{1570}}\right)$ to give the burning rate.

With the boundary conditions at 1570° K taken as the cold boundary, the analytical solution appropriate to gaseous conditions may be obtained; that is, the energy equation (eq. $(10_B)$), the continuity equation (eq. $(11_B)$), the equilibrium equations (eqs. $(5_B)$), and the pressure equation (eq. $(3_B)$) may be iterated as in the general case and the carbon case.

This solution produces a plot of the partial pressure of each component against temperature, as shown in figure 2(b). The appearance of the closed loop in the plot of the partial pressure of boric oxide is solely the result of the equilibria and the plot, and has no physical significance in itself.

The burning rate $W_f$ can be obtained using the continuity equation for boron by substituting the diffusion equations and integrating. This yields

$$\frac{W_f}{4\pi}\left(\frac{1}{r_A} - \frac{1}{r_{1570}}\right) = \sum_{\Delta T}^{1570 \text{ to } T_A} x\left(\delta_B \Delta p_B + 2\delta_{B_2}\Delta p_{B_2} + \delta_{BO}\Delta p_{BO} + 2\delta_{B_2O_3}\Delta p_{B_2O_3}\right) \tag{16_B}$$

to which may be added the right side of equation $(35_B)$ to obtain $\frac{W_f}{4\pi}\left(\frac{1}{r_A} - \frac{1}{r_C}\right)$. $\frac{W_f}{4\pi r_A}$ is obtained by letting $\frac{1}{r_C}$ approach zero.

The structure of the boron flame can be deduced from the curves of the partial pressure, as discussed in connection with equation (17).

## Graphical Method for Burning Rate

Because the assumption is made that $p_B$, $p_{B_2}$, and $p_{BO}$ are equal to zero at the 1570° K boundary condition, that $p_{B_2O_3,1570}$ is constant, and that the inner boundary is defined by an equilibrium, the quantity obtained in equation $(16_B)$ is determined by the partial pressure of oxygen at 1570° K. The analytical solution is carried out for a series of such oxygen values. Figure 4 is a graph showing integrated values for $\frac{W_f}{4\pi}\left(\frac{1}{r_A} - \frac{1}{r_{1570}}\right)$ from equation $(16_B)$. The straight-line appearance seems coincidental.

Figures 4, 5, and 6 permit a rapid evaluation of the burning rate for wide ranges of ambient partial pressure of oxygen (see example in RESULTS section). In essence

$$\frac{W_f}{4\pi r_A} = f(T_C, p_{O_2,C})$$

$$= \frac{W_f}{4\pi}\left(\frac{1}{r_A} - \frac{1}{r_{1570}}\right) + \frac{W_f}{4\pi}\left(\frac{1}{r_{1570}} - \frac{1}{r_C}\right)$$

$$\equiv g(p_{O_2,1570}) + h(T_C)$$

where $p_{O_2,1570}$ is obtained from $p_{O_2,C}$ and $T_C$ by figure 5. $h(T_C)$ represents the quantity plotted in figure 6, and $g(p_{O_2,1570})$ that in figure 4.

4076

4076

CE-5 back

# APPENDIX C

## REDUCTION OF GENERAL EQUATIONS TO SIMPLIFIED EQUATIONS

The calculations developed in the GENERAL EQUATIONS section and applied to carbon as an example and to boron in appendix B require no assumptions about any internal boundary conditions of the flame zone. Indeed, the structure of the flame follows as a consequence of the assumptions made about equilibrium and diffusion. When certain assumptions are made about the flame front, in terms of the models in figure 1, the general equations can be simplified. The simplification is both in the form of and the number of equations involved. The resulting simplified equations are those used previously for hydrocarbons (refs. 1 and 5) and for magnesium (ref. 6). An infinitesimal flame front (boundary B, fig. 1(a)), where the concentrations of fuel and oxygen are zero, is used for the hydrocarbons and boron. A flame front of finite thickness (region BB', fig. 1(b)) involving a high-temperature diffusion zone is used for magnesium. In both cases, the fuel surface is assumed to be at its boiling point; $T_A = T_{b.p.}$.

### Hydrocarbons and Boron

The diffusion equation (eq. (2b)) for oxygen may be written

$$\frac{W_{O_2}}{4\pi r^2} = \frac{-D_{O_2}}{RT}\frac{dp_{O_2}}{dr} = \frac{-n_{O_2}W_f}{4\pi r^2} \tag{2b$_H$}$$

because $W_{O_2} = -n_{O_2}W_{f_2}$ in the over-all process.

The energy equation (eq. (7)) may be written in the form

$$W_f\left[H_{f_o} - H_f + n_{O_2}H_{O_2} - n_pH_p\right] = -4\pi r^2 \kappa \frac{dT}{dr} \tag{7$_H$}$$

Oxygen and product terms may be written so as to allow for dissociation in order to maintain realistic temperatures; the most practical assumptions (ref. 5) are atomic homogeneity (a constant ratio among the atom species regardless of their chemical arrangement) and chemical equilibrium among the molecular species. From the composition-temperature information, estimates of the enthalpy-temperature function can be obtained. Variations in the enthalpy function in equation ($7_H$) produce variations in $T_B$ from equation ($40_H$), but such errors tend to cancel out in the graphical integration of equation ($41_H$), where the same enthalpy function appears.

Now if the conditions that $p_{O_2} = p_f = 0$ at the flame-front boundary are applied to the energy equation, some simplifications occur. For the AB region inside the flame front, there is no net flow $W$ of any component other than fuel. The fuel is assumed to proceed uncracked and unreacted to the flame front; therefore, only the fuel contributes to the enthalpy term. The energy equation for the region AB inside the flame front becomes

$$W_f\left[H_{f_o} - H_f\right] = W_f\left[\Delta H + L + H_f - H_{f,T_A}\right] = -4\pi r^2 \varkappa_{AB} \frac{dT}{dr} \qquad (37_H)$$

In the region BC outside the flame front, oxygen diffuses inward, and products diffuse out; the energy equation may be written as

$$W_f\left[H_{f_o} + n_{O_2}(H_{O_2} - H_{O_2,C}) - n_p(H_p - H_{p,C}) + n_{O_2}H_{O_2,C} - n_pH_{p,C}\right] = -4\pi r^2 \varkappa_{BC} \frac{dT}{dr} \qquad (38_H)$$

or

$$W_f\left[Q + n_{O_2}(H_{O_2} - H_{O_2,C}) - n_p(H_p - H_{p,C})\right] = -4\pi r^2 \varkappa_{BC} \frac{dT}{dr} \qquad (39_H)$$

where $Q$ is the heat of combustion of the fuel particle at its initial temperature with oxygen at $T_C$ to give products at $T_C$. The terms $n_{O_2}(H_{O_2} - H_{O_2,C})$ and $n_p(H_p - H_{p,C})$ (decomposed into their dissociation products where necessary) are a correction to the quantity of heat to be conducted. In equations $(37_H)$ and $(39_H)$, the quantity in brackets is the amount of heat that must be conducted through each temperature region in the steady state for each mole of fuel consumed.

In the outer BC zone, the diffusion equation for oxygen (eq. $(2b_H)$) and the energy equation (eq. $(39_H)$) yield

$$\frac{D_{O_2}}{n_{O_2}RT\varkappa_{BC}} \int_{p_{O_2,C}}^{p_{O_2,B}=0} dp_{O_2} = \int_{T_C}^{T_B=?} \frac{dT}{\left[Q + n_{O_2}(H_{O_2} - H_{O_2,C}) - n_p(H_p - H_{p,C})\right]} \qquad (40_H)$$

The quantity $D_{O_2}/\varkappa_{BC}T$ is essentially independent of temperature. With the enthalpy function known, the right side of equation $(40_H)$ can be evaluated graphically to determine $T_B$.

4076

The energy equations (eqs. ($37_H$) and ($39_H$)) can be integrated in their respective zones to yield

$$\frac{W_f}{4\pi}\left(\frac{1}{r_A} - \frac{1}{r_C}\right) = \int_{T_A}^{T_B} \frac{\varkappa_{AB}dT}{\left[\Delta H + L + H_f - H_{f,A}\right]} + \int_{T_C}^{T_B} \frac{\varkappa_{BC}dT}{\left[Q + n_{O_2}(H_{O_2} - H_{O_2,C}) + n_p(H_p - H_{p,C})\right]} = \underline{B} + \underline{C} \tag{$41_H$}$$

$$= \underline{B} + \underline{C}$$

4076

By using the value of $T_B$ obtained from equation ($40_H$), the two integrals on the right side of equation ($41_H$) may be integrated graphically. Values of $\varkappa$ must be estimated because the composition is not determined; in the AB zone $\varkappa_{AB}$ is appropriately taken as that of the fuel; in the BC zone $\varkappa_{BC}$ is taken as that of the inert present in the ambient atmosphere. Errors made in the estimation of $n$ in the enthalpy function and in the selection of $\varkappa$ for the evaluation of $T_B$ in equation ($40_H$) tend to cancel out when $W_f$ is evaluated by equation ($41_H$).

As $1/r_C \rightarrow 0$, equation ($41_H$) yields the burning rate $W_f/4\pi r_A$. The only information easily deduced about structure from this calculation is the value of $r_B$, which can be determined from $W_f$ and the value of either of the two integrals. A more compact expression is

$$\frac{r_B}{r_A} = \frac{\underline{B} + \underline{C}}{\frac{r_A}{r_C}\underline{B} + \underline{C}} = \frac{\underline{B} + \underline{C}}{\underline{C}} \tag{$42_H$}$$

The form $(\underline{B} + \underline{C})/\underline{C}$ arises as $1/r_C \rightarrow 0$.

Values for the burning rate of a typical hydrocarbon (isooctane) are included in the RESULTS section. (They were obtained by use of the integrals $\underline{B}$ and $\underline{C}$ from figures 8 and 9 and $T_B$ from figure 10 of reference 5.) The values of the integrals in reference 5 are converted to the units used in this report, (moles of fuel)/(cm)(sec), when multiplied by 0.1304 $(g/lb)(cm/ft)^{-1}(g/mole)^{-1}$.

## Magnesium

High-temperature dissociation data are not available for magnesium oxide. Further, there is some evidence that the oxide dissociates completely upon vaporization (this implies that the heat of vaporization is

equal to the heat of reaction at the boiling point). Therefore, for magnesium, the flame front of infinitesimal thickness was replaced (ref. 6) by a high-temperature zone of diffusion and reaction at the boiling point of the oxide (region BB', fig. 1(a)).

The energy equation may be written

$$\left.\begin{aligned} W_f H_{f_o} - W_{Mg} H_{Mg} - W_{O_2} H_{O_2} - W_{MgO} H_{MgO} &= -4\pi r^2 \varkappa \frac{dT}{dr} \\ W_f\left[H_{f_o} - H_{Mg} + n_{O_2} H_{O_2} - n_{MgO} H_{MgO}\right] &= -4\pi r^2 \varkappa \frac{dT}{dr} \end{aligned}\right\} \qquad (7_{Mg})$$

4076

Dissociation is considered only in the reaction zone.

In the AB region inside the reaction zone, there is no net flow of any component except fuel. Products are presumed to pass outward (despite minor oxide deposits on the ribbon in the experimental case). The energy equation in the AB zone becomes

$$W_f\left[\Delta H + L + H_{Mg} - H_{Mg,A}\right] = 4\pi r^2 \varkappa_{AB} \frac{dT}{dr} \qquad (37_{Mg})$$

In the region B'C outside the reaction zone, oxygen diffuses inward, and MgO floats out. The energy equation may be written, analogously to that for the hydrocarbon case, as

$$W_f\left[Q + n_{O_2}(H_{O_2} - H_{O_2,C}) - n_{MgO}(H_{MgO} - H_{MgO,C})\right] = -4\pi r^2 \varkappa_{B'C} \frac{dT}{dr} \qquad (39_{Mg})$$

Because of the condensed product, the diffusion equation for oxygen reduces to the equation for the diffusion of oxygen through a stagnant film of the ambient inert gas (form of eq. (D6), appendix D):

$$\frac{W_{O_2}}{4\pi r^2} = \frac{-D_{O_2} P}{RT(P - p_{O_2})} \frac{dp_{O_2}}{dr} \qquad (43_{Mg})$$

The diffusion equations for oxygen and the energy equation for the outer B'C zone, combined and integrated, yield

$$\frac{D_{O_2}}{n_{O_2}RT\varkappa_{B'C}}\int_{p_{O_2,C}}^{p_{O_2,B'}=?p}\frac{dp_{O_2}}{P-p_{O_2}}=\int_{T_C}^{T_{B'}=T_{b.p.}}\frac{dT}{\left[Q+n_{O_2}(H_{O_2}-H_{O_2,C})-n_p(H_p-H_{p,C})\right]} \tag{44$_{Mg}$}$$

4076

In this case, the graphical integration yields the partial pressure of oxygen at the B' boundary rather than the temperature of the flame front, as in the hydrocarbon case (eq. (40$_H$)). $D_{O_2}/T\varkappa_{B'C}$ is again assumed to be independent of temperature.

In the high-temperature diffusion zone (BB') combining the continuity equations

$$\left.\begin{aligned} 2W_{O_2} + W_{MgO} &= 0 \\ W_{Mg} + W_{MgO} &= W_f \end{aligned}\right\} \tag{1$_{Mg}$}$$

with the energy equation (7$_{Mg}$) yields

$$W_{Mg}(H_{f_o} - H_{Mg}) + 2W_{O_2}\left(H_{MgO} - H_{f_o} - \frac{1}{2}H_{O_2}\right) = -4\pi r^2\varkappa\frac{dT}{dr} \tag{45$_{Mg}$}$$

In the BB' region of high-temperature diffusion, the temperature gradient is zero;

$$\left.\begin{aligned} W_{Mg} &= -2W_{O_2}\left(\frac{Q_{3200}}{\Delta H + L + H_{Mg} - H_{Mg,A}}\right) \equiv -2\mathscr{H}W_{O_2} \\ &\text{and similarly} \\ W_f &= -2(\mathscr{H}+1)W_{O_2} \end{aligned}\right\} \tag{46$_{Mg}$}$$

Here $Q_{3200}$ indicates the heat of combustion of magnesium at $T_o$ to form condensed MgO at 3200° K. The factor $\mathscr{H} \cong 2.0$ does not appear in reference 6. It may be regarded as the ratio of the amounts of MgO condensed at the outer and inner boundaries of the BB' zone.

In the high-temperature region, the diffusion equations for oxygen and magnesium are in the form of equations (2a). Both diffusion equations and both forms of equation $(46_{Mg})$ combine to yield

$$\frac{W_f}{4\pi r^2} = \frac{D_{O_2}P}{RT}\,\frac{(2\mathscr{H} + 2)}{P + (2\mathscr{H} - 1)p_{O_2}}\,\frac{dp_{O_2}}{dr} \tag{$47_{Mg}$}$$

Equation $(47_{Mg})$ is integrated over the boundary conditions $p_{O_2} = p_{O_2,B'}$ at $r = r_{B'}$ and $p_{O_2} = 0$ at $r = r_B$. In reference 6, the factor $(2\mathscr{H} + 2)/(2\mathscr{H} - 1) \cong 2.0$ does not appear in the integrated form of the diffusion equation; rather the factor is $1/n_{O_2} = 2$. The introduction of $\mathscr{H}$ from the general equations, instead of the use of equation $(43_{Mg})$ for the diffusion of oxygen in the high-temperature zone, does result in some modification in the dependence of the burning rate upon ambient partial pressure of oxygen; the original formulation, which now must be regarded as semiempirical, fits the experimental results somewhat more satisfactorily.

Finally, the burning rate is obtained by adding the integrated forms of equations $(37_{Mg})$, $(39_{Mg})$, and $(47_{Mg})$. As $1/r_C \to 0$,

$$\frac{W_f}{4\pi r_A} = \int_{T_A}^{T_B} \frac{\varkappa_{AB}}{\left[H_{Mg} - H_{f_o}\right]}\,dT + \frac{D_{O_2}P}{RT}\,\frac{2\mathscr{H} + 2}{2\mathscr{H} - 1}\ln\frac{P + (2\mathscr{H} - 1)p_{O_2,B'}}{P} +$$

$$\int_{T_C}^{T_B} \frac{\varkappa_{B'C}}{\left[Q + n_{O_2}(H_{O_2} - H_{O_2,C}) - n_p(H_p - H_{p,C})\right]}\,dT = \underline{B} + \underline{B'} + \underline{C} \tag{$48_{Mg}$}$$

Each term of equation $(48_{Mg})$ is positive with the logarithmic term dominating, particularly in oxygen-rich atmospheres. Equation $(44_{Mg})$ shows a strong dependence of $p_{O_2,B'}$ upon $p_{O_2,C}$, the ambient partial pressure of oxygen; this shows up in turn in equation $(48_{Mg})$ as a strong dependence of $W_f$ upon $p_{O_2,B'}$. This is consistant with the experimental evidence for ambient atmospheres covering a range of 15 to 100 percent $O_2$ (ref. 6).

4076

# APPENDIX D

## DERIVATION OF APPROXIMATE DIFFUSION EQUATIONS FOR MULTICOMPONENT MIXTURES

General equations for diffusion in multicomponent mixtures are presented in reference 10 (pp. 516-520). If external forces, pressure gradients, and thermal diffusion are neglected, equations (8.1-3) of reference 10 become:

$$\sum_{j=1}^{\nu} \frac{n_i n_j}{n^2 D_{ij}} (\overline{V}_j - \overline{V}_i) = \frac{d}{dr}\left(\frac{n_i}{n}\right) \qquad i = 1,2, \ldots, \nu - 1 \qquad \text{(D1)}$$

where $n_i$ and $n_j$ are concentrations of species $i$ and $j$ in molecules per cubic centimeter; $n$ is the total number of molecules per cubic centimeter; $\overline{V}_j$ and $\overline{V}_i$ are diffusion velocities, in centimeters per second; $D_{ij}$ is the binary diffusion coefficient; and $r$ is distance in centimeters. In a $\nu$ component mixture, only $\nu - 1$ of these equations are independent.

The diffusion velocity $\overline{V}_i$ or $\overline{V}_j$ is related to the flux of molecules $G_i$ or $G_j$ (moles/(sq cm)(sec)) through a unit area normal to the direction of diffusion. Assume the gases obey the ideal gas law; then

$$\overline{V}_j = \frac{G_j}{x_j} \frac{RT}{P}$$

where $x_j = n_j/n$ is the mole fraction of component $j$. A similar equation relates $\overline{V}_i$ and $G_i$.

Equations (D1) become

$$x_i \sum_{j=1}^{\nu} \frac{G_j}{\beta_{ij}} - G_i \sum_{j=1}^{\nu} \frac{x_j}{\beta_{ij}} = \frac{dx_i}{dr} \qquad i = 1,2, \ldots, \nu - 1 \qquad \text{(D2)}$$

where $\beta_{ij} = D_{ij}P/RT$. If, as an approximation, it is assumed that the binary diffusion coefficients of component $i$ into each of the other

components of the mixture are equal, then $\beta_{i_1} = \beta_{i_2} = \ldots = \beta_{i_j} = \ldots = \beta_{i_\nu} \equiv \beta_i$, and

$$x_i \sum_{j=1}^{\nu} G_j - G_i = \beta_i \frac{dx_i}{dr}$$

or

$$x_i \sum_{j=1}^{\nu-1} G_j - G_i = \beta_i \frac{dx_i}{dr} - x_i G_\nu$$

$$= C_i \qquad i = 1,2, \ldots, \nu - 1 \tag{D3}$$

where $G_\nu$ is the flow of the component for which no equation has been written.

It is convenient to solve these equations (by means of determinants) for $G_i$ as a function of all the $x_j$ and $C_j$:

$$G_i = -C_i - \frac{x_i \sum_{j=1}^{\nu-1} C_j}{1 - \sum_{j=1}^{\nu-1} x_j}$$

$$= -\left(\beta_i \frac{dx_i}{dr} + \frac{x_i}{x_\nu} \sum_{j=1}^{\nu-1} \beta_j \frac{dx_j}{dr}\right) + \frac{x_i}{x_\nu} G_\nu$$

$$= -\left(\frac{D_i}{RT} \frac{dp_i}{dr} + \frac{p_i}{p_\nu} \sum_{j=1}^{\nu-1} \frac{D_i}{RT} \frac{dp_i}{dr}\right) + \frac{p_i}{p_\nu} G_\nu \qquad i = 1,2, \ldots, \nu - 1 \tag{D4}$$

These equations are strictly valid only in mixtures where binary diffusion coefficients between all the pairs of species are equal, that is, in binary mixtures.

When there is an inert gas present in the system, it is stagnant (its flow is zero). In problems concerning the burning of liquid or solid fuels in air, nitrogen is such a diluent, provided formation of nitrogen atoms and NO molecules is neglected. In this event it is convenient to select $G_\nu = G_{N_2} = 0$. (This is not convenient if the amount of inert gas is small, because as $p_\nu \to 0, p_i/p_\nu \to \infty$.) Equation (D4) then becomes

$$-G_i = \frac{D_i}{RT}\frac{dp_i}{dr} + \frac{p_i}{p_{N_2}}\sum_{j=1}^{\nu-1}\frac{D_j}{RT}\frac{dp_j}{dr} \tag{D5}$$

In a binary mixture, $p_{N_2} = P - p_i$, and equation (D5) becomes

$$-G_i = \frac{1}{\left(1 - \frac{p_i}{P}\right)}\frac{D_i}{RT}\frac{dp_i}{dr} \tag{D6}$$

which is the familiar equation for diffusion of one gas through a stagnant film of a second gas (ref. 11).

Finally, when the concentrations of diffusing gases are small relative to the amount of inert gas, the second term may be neglected ($p_i/p_\nu \to 0$). In this event the simplest form of diffusion equation occurs:

$$-G_i = \frac{D_i}{RT}\frac{dp_i}{dr} \tag{D7}$$

which is the same form as the equation for equimolar counter diffusion in a binary mixture.

4076

CE-6 back

## APPENDIX E

## ESTIMATION OF $\delta_i$ FOR CARBON AND BORON COMBUSTION

The quantities $\delta_i$ are defined by

$$\delta_i \equiv \frac{D_i}{\varkappa RT} \tag{E1}$$

4076

where $D_i$ is the diffusion coefficient for component $i$ into the gas mixture, and $\varkappa$ is the thermal conductivity. For the combustion of carbon and boron in air the properties of the gas mixture exclusive of component $i$ are approximated by those of nitrogen. From the expressions for diffusion coefficient and thermal conductivity presented in reference 10,

$$\delta_i = \frac{D_{i-N_2}}{\varkappa_{N_2}RT} = \frac{0.644}{P\left(1 + \frac{\sigma_i}{\sigma_{N_2}}\right)^2}\sqrt{\frac{M_i + M_{N_2}}{2M_i}}\,\frac{\Omega_{N_2}^{(2,2)*}}{\Omega_{i-N_2}^{(2,2)*}}\,\frac{A_{i-N_2}^*}{\left(\frac{4}{15}\frac{C_{p_{N_2}}}{R} + \frac{1}{3}\right)} \tag{E2}$$

where $A_{i-N_2}^* = \Omega_{i-N_2}^{(2,2)*}\Big/\Omega_{i-N_2}^{(1,1)*}$.

The ratio $\Omega_{N_2}^{(2,2)*}\Big/\Omega_{i-N_2}^{(2,2)*}$ is further approximated as equal to unity. The quantity $A_{i-N_2}^*$ is close to 1.1 for a Lennard-Jones (6-12) interaction potential between molecules (ref. 10). The heat capacity of nitrogen has been taken at 2000° K (ref. 7) (a reasonable mean temperature). With these approximations

$$\delta_i = \frac{0.337}{P\left(1 + \frac{\sigma_i}{\sigma_{N_2}}\right)^2}\sqrt{1 + \frac{M_{N_2}}{M_i}} \tag{E3}$$

In order to estimate $\delta_i$ values, the molecular diameters for the atoms and molecules involved must be obtained.

For carbon combustion, $\sigma$ values for $N_2$, $O_2$, CO, and $CO_2$ were taken from reference 10. For atomic oxygen, the diameter was estimated assuming the same mean density of matter in the atom as in the molecule, that is,

$$\sigma_{atom} = \sqrt[3]{\frac{1}{2}}\,\sigma_{diatomic\ molecule} = 0.794\,\sigma_{molecule} \tag{E4}$$

(This method probably underestimates somewhat the diameters of atoms, since the electron density of an atom is usually lower than that of the corresponding diatomic molecule.) Diameters chosen and the corresponding $\delta$ values at atmospheric pressure are shown in the following table:

| Molecule | Diameter, Å | Diameter obtained from - | $\delta$ at 1 atmosphere (eq. (E3)) |
|---|---|---|---|
| $N_2$ | 3.749 | Ref. 10 | 0.1192 |
| $O_2$ | 3.541 | Ref. 10 | .1220 |
| CO | 3.706 | Ref. 10 | .1205 |
| $CO_2$ | 3.897 | Ref. 10 | .1037 |
| O | 2.810 | Eq. (E4) | .1827 |

For boron combustion, diameters of $N_2$, $O_2$, $B_2$, BO, O, B, and $B_2O_3$ must be obtained. (Literature values exist only for nitrogen and oxygen.) It was found, however, that a plot of the quotient of molecular diameter (ref. 10) and internuclear distance (ref. 12) against internuclear distance for a number of diatomic molecules gave a smooth correlation. This is shown in figure 7. From this correlation and the known internuclear distances of $N_2$, $O_2$, $B_2$, and BO (ref. 12) molecular diameters for the diatomic molecules were obtained. Atomic diameters for B and O were then calculated from equation (E4). The diameter of $B_2O_3$ was estimated from the density of crystalline $B_2O_3$, with the molecules assumed to occupy 74 percent of the crystal volume (closest packing of spheres). Results are shown in the following table:

| Molecule | Diameter, Å | Diameter obtained from - | $\delta$ at 1 atmosphere (eq. (E3)) |
|---|---|---|---|
| $N_2$ | 3.70 | Fig. 7 and internuclear distances of ref. 12 | 0.1192 |
| $O_2$ | 3.52 | Fig. 7 and internuclear distances of ref. 12 | .1212 |
| $B_2$ | 3.82 | Fig. 7 and internuclear distances of ref. 12 | .1238 |
| BO | 3.50 | Fig. 7 and internuclear distances of ref. 12 | .1273 |
| O | 2.80 | Eq. (E4) | .1812 |
| B | 3.04 | Eq. (E4) | .1925 |
| $B_2O_3$ | 4.50 | Density of $B_2O_3$ (crystal) = 1.805, and assumption that 74 percent of volume is occupied | .0812 |

## REFERENCES

1. Spalding, D. B.: Combustion of Fuel Particles. Fuel, vol. XXX, no. 6, June 1951, pp. 121-130.

2. Godsave, G. A. E.: Studies of the Combustion of Drops in a Fuel Spray - The Burning of Single Drops of Fuel. Fourth Symposium (International) on Combustion, The Williams & Wilkins Co. (Baltimore), 1953, pp. 818-830.

3. Goldsmith, M., and Penner, S. S.: On the Burning of Single Drops of Fuel in an Oxidizing Atmosphere. Tech. Rep. No. 2, GALCIT, Nov. 1953. (Contract DA 04-495-Ord-446.)

4. Wise, Henry, Lorell, Jack, and Wood, Bernard J.: The Effects of Chemical and Physical Parameters on the Burning Rate of a Liquid Droplet. Fifth Symposium (International) on Combustion, Reinhold Pub. Corp., 1955, pp. 132-141.

5. Graves, Charles C.: Burning Rates of Single Fuel Drops and Their Application to Turbojet Combustion Process. NACA RM E53E22, 1953.

6. Coffin, Kenneth P.: Burning Times of Magnesium Ribbons in Various Atmospheres. NACA TN 3332, 1954. (See also Fifth Symposium (International) on Combustion, Reinhold Pub. Corp., 1955, pp. 267-276.)

7. Huff, Vearl N., Gordon, Sanford, and Morrell, Virginia E.: General Method and Thermodynamic Tables for Computation of Equilibrium Composition and Temperature of Chemical Reaction. NACA Rep. 1037, 1951. (Supersedes NACA TN's 2113 and 2161.)

8. Milne, William Edmund: Numerical Calculus. Princeton Univ. Press, 1949.

9. Nathan, Charles C.: The Heat of Combustion of Boron and of Lithium Borohydride. Univ. Pitts. Bull., vol. 46, no. 10, June 5, 1950.

10. Hirschfelder, Joseph O., Curtiss, Charles F., and Bird, R. Byron: Molecular Theory of Gases and Liquids. John Wiley & Sons, Inc., 1954.

11. Sherwood, Thomas K., and Pigford, Robert L.: Absorption and Extraction. Second ed., McGraw-Hill Book Co., Inc., 1952.

12. Herzberg, Gerhard: Spectra of Diatomic Molecules. Second ed., D. Van Nostrand Co., Inc., 1950.

4076

4076

TABLE I. - COMPUTED BURNING RATES OF VARIOUS SUBSTANCES

[Temperature, 300° K; air at 1 atmosphere.]

| | Burning rate, $W_f$ | | | Evaporation constant, $\beta'$, $\frac{\text{sq microns}}{\text{sec}}$ | Lifetime of 1-micron particle, $t_l$, sec |
|---|---|---|---|---|---|
| | $\frac{\text{moles}}{(\text{cm})(\text{sec})}$ | $\frac{\text{gm}}{(\text{cm})(\text{sec})}$ | $\frac{\text{cal}}{(\text{cm})(\text{sec})}$ | | |
| Isooctane[a] | $0.86\times10^{-5}$ | $99\times10^{-5}$ | 10.5 | $1.11\times10^{6}$ | $0.90\times10^{-6}$ |
| Magnesium[a] | 3.97 | 97 | 5.7 | .444 | 2.25 |
| Boron | | | | | |
| [a]Case A | 1.31 | 14.2 | 1.98 | .0492 | 20.3 |
| [a]Case B | 1.79 | 19.4 | 2.70 | .0673 | 14.8 |
| Analytical | 1.27 | 13.7 | 1.92 | .0477 | 21.0 |
| Carbon | | | | | |
| Numerical | 1.05 | 12.7 | 1.02 | .0505 | 19.8 |
| Analytical | 1.10 | 13.2 | 1.07 | .053 | 18.9 |

[a]Simplified calculation.

TABLE II. - EFFECTS OF AMBIENT TEMPERATURE AND AMBIENT PARTIAL PRESSURE OF OXYGEN ON BURNING RATE OF BORON

[Pressure, 1 atmosphere.]

| Temperature, °K | Oxygen concentration, percent | Burning rate, moles/(cm)(sec) | | |
|---|---|---|---|---|
| | | Extended calculation | Simplified calculation (eq. ($4l_H$)) | |
| | | | Case A | Case B |
| 300 | 20.95 | $12.7\times10^{-6}$ | $13.1\times10^{-6}$ | $17.9\times10^{-6}$ |
| 800 | 20.95 | 13.2 | 13.1 | 19.1 |
| 1300 | 20.95 | 14.5 | 13.0 | 20.4 |
| 800 | 15.00 | 8.2 | 11.2 | 12.1 |

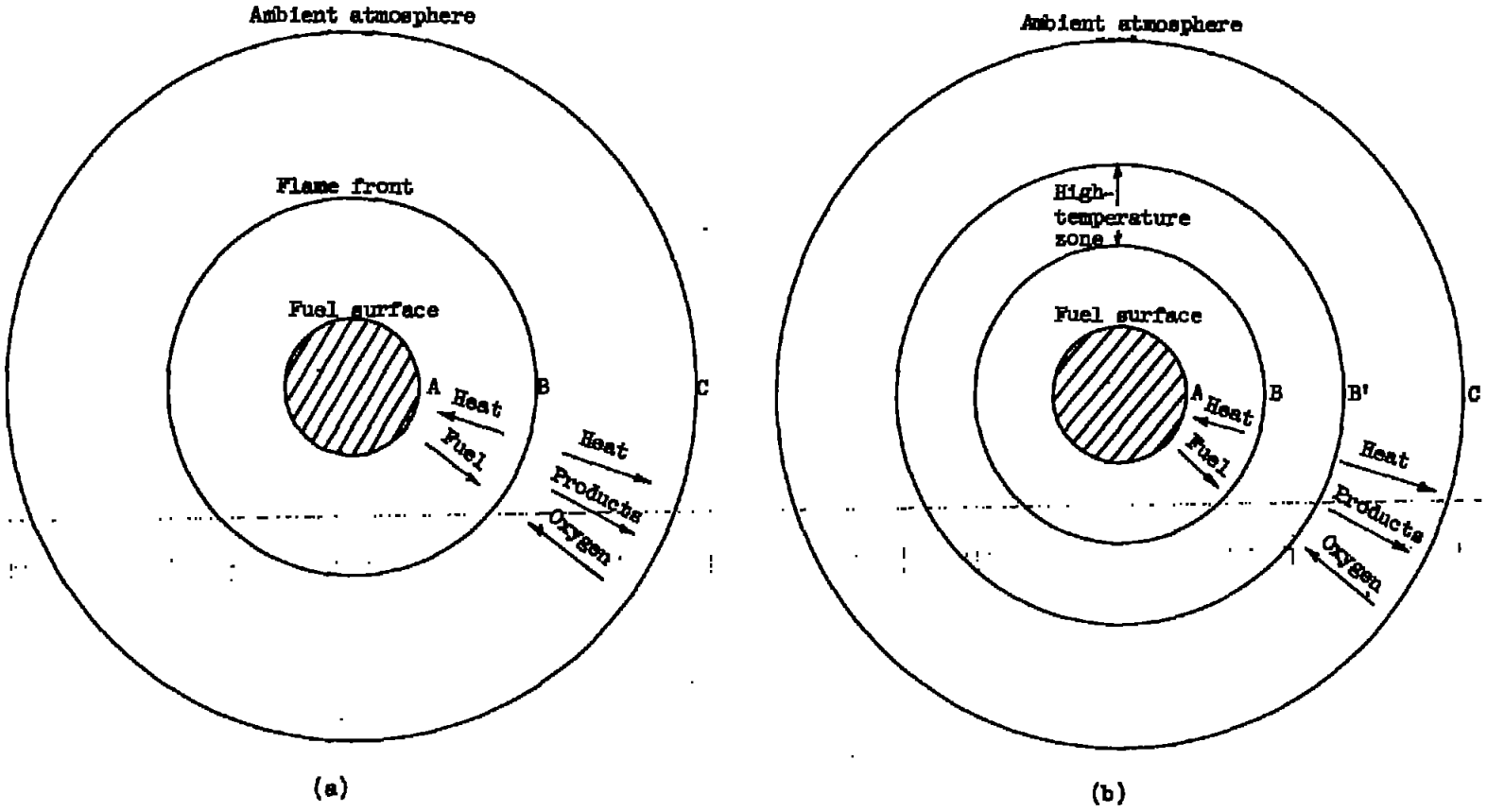


Figure 1. - Cross-sectional models of burning fuel particles.

4076

CE-7

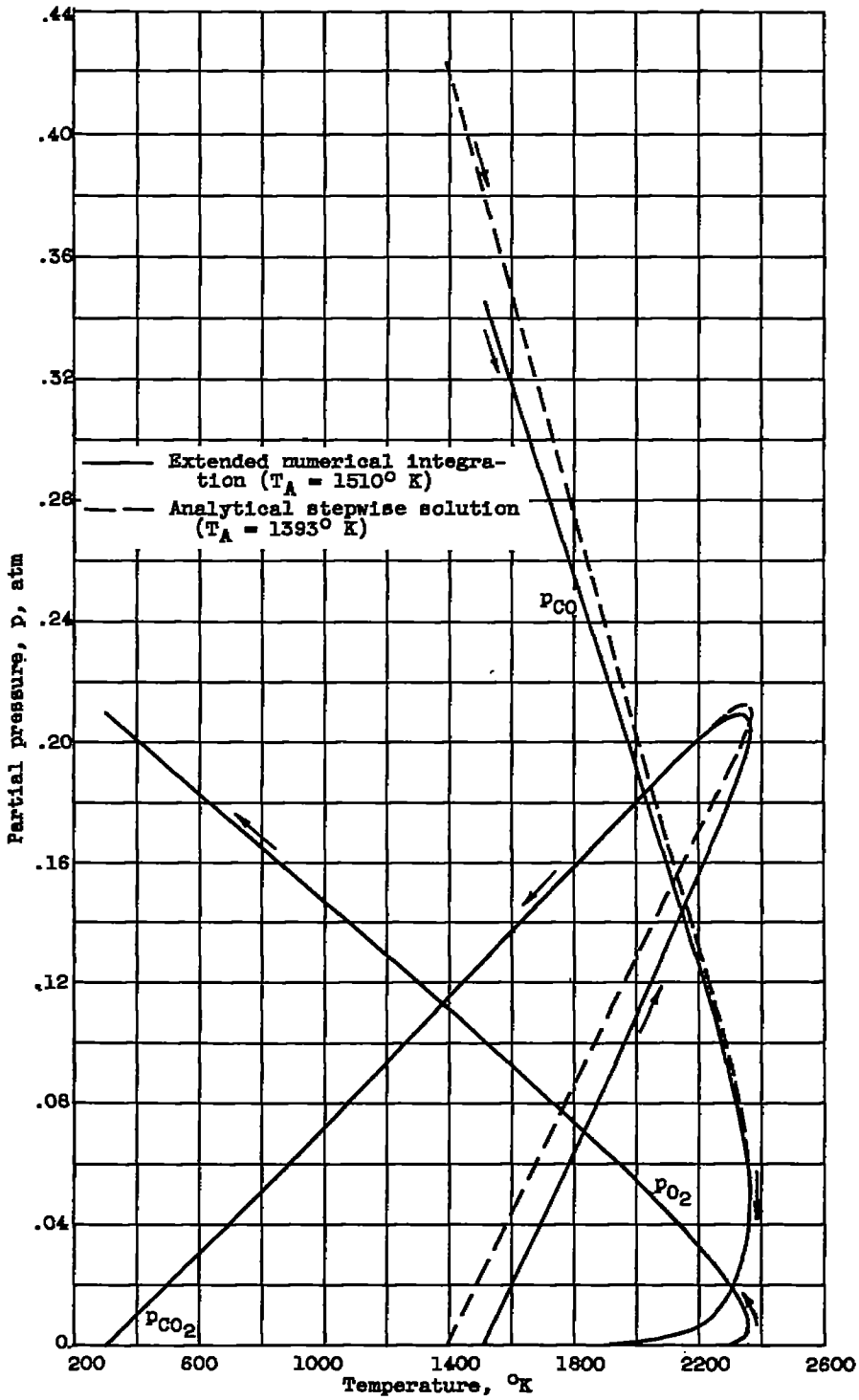


(a) Carbon. Maximum partial pressure of oxygen atoms, $0.8 \times 10^{-3}$ atmosphere (not plotted).

Figure 2. - Pressure-temperature curves for burning in air. Arrows indicate outward direction.

4076

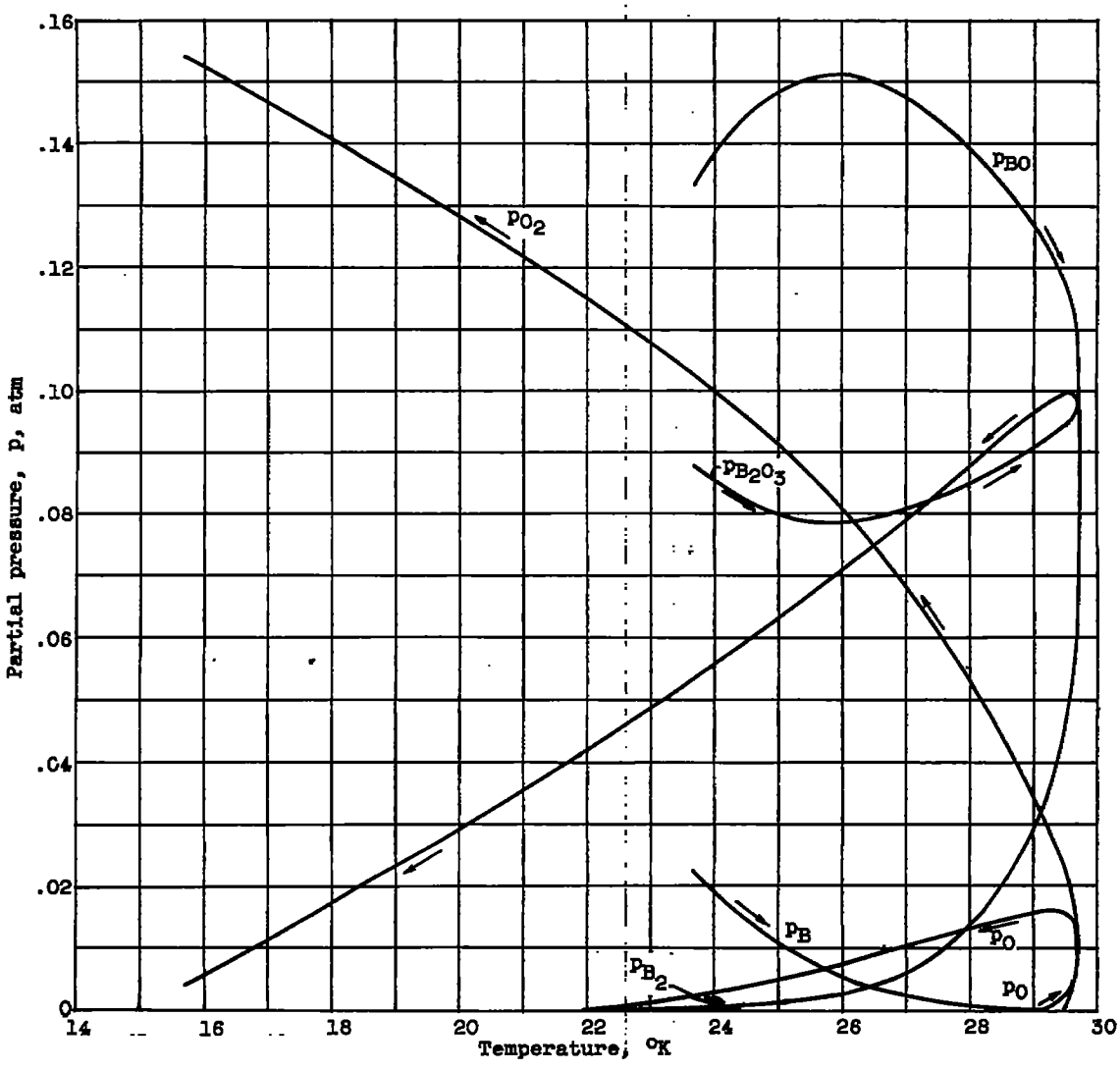


(b) Boron.

Figure 2. - Concluded. Pressure-temperature curves for burning in air. Arrows indicate outward direction.

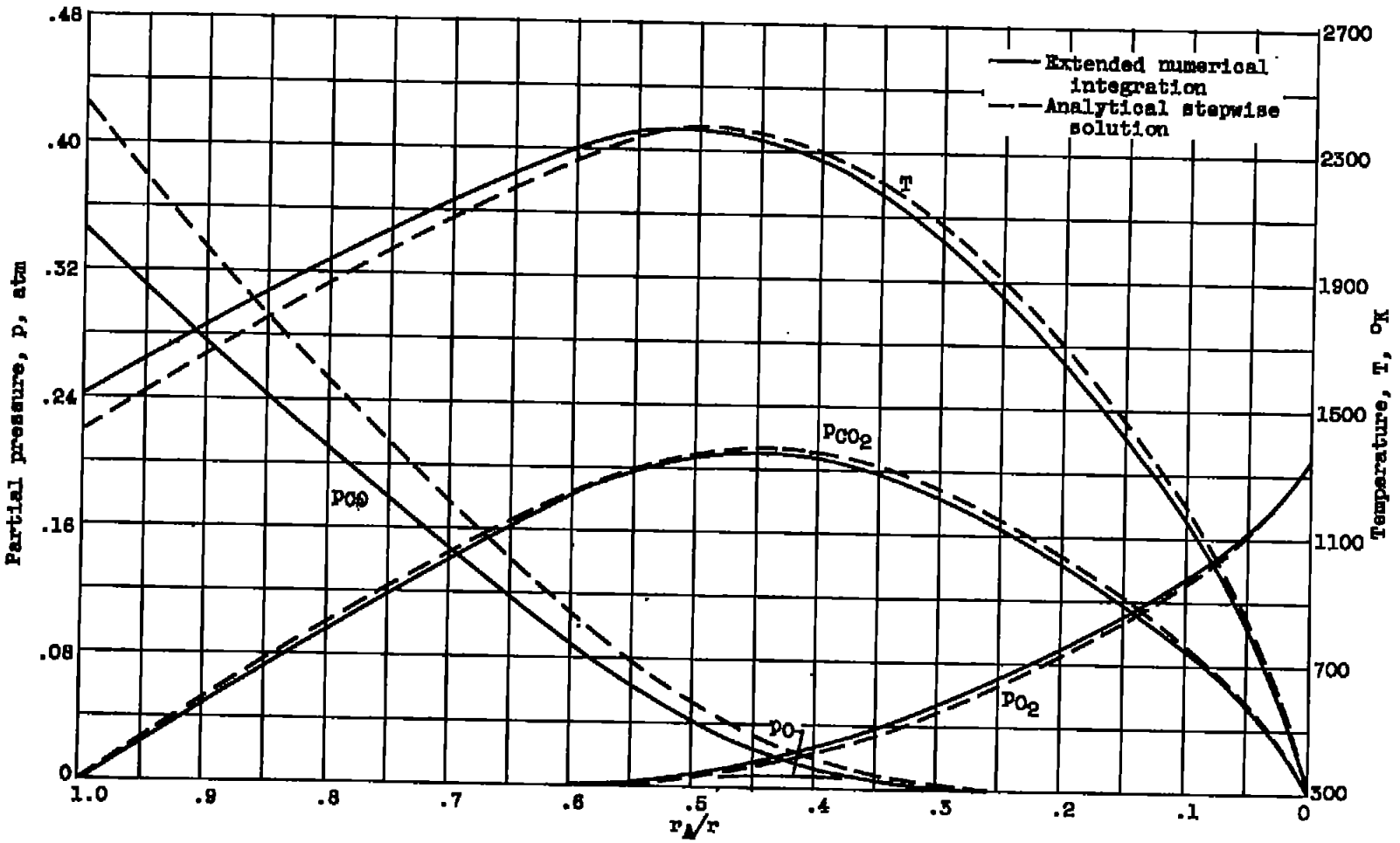


(a) Carbon.

Figure 3. - Flame structure of particles burning in air. r, distance from center of particle; $r_A$, radius of particle.

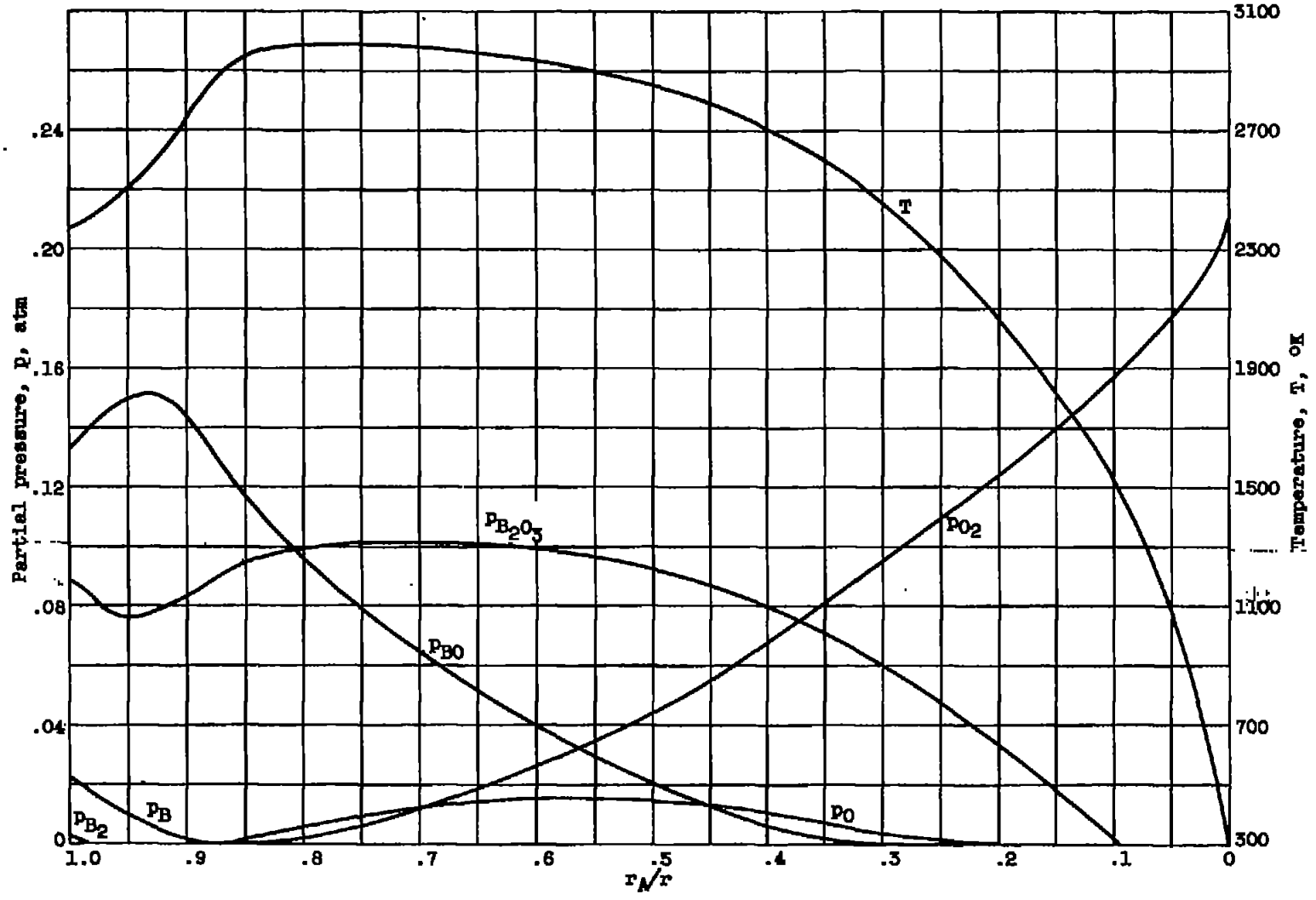


(b) Boron.

Figure 3. - Concluded. Flame structure of particles burning in air. r, distance from center of particle; $r_A$, radius of particle.

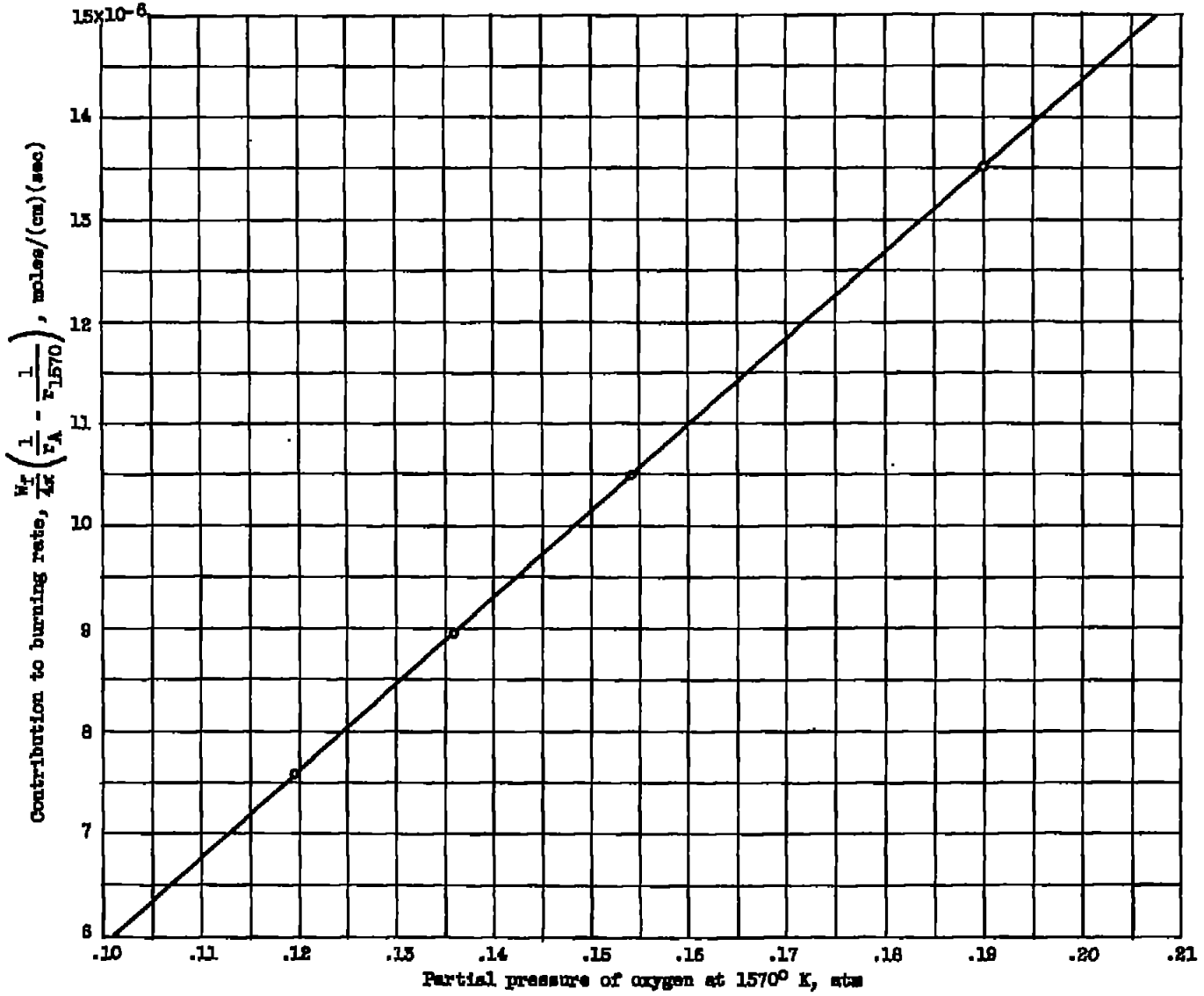


Figure 4. - Contribution to burning rate for regions above 1570° K (eq. ($18_B$), appendix B).

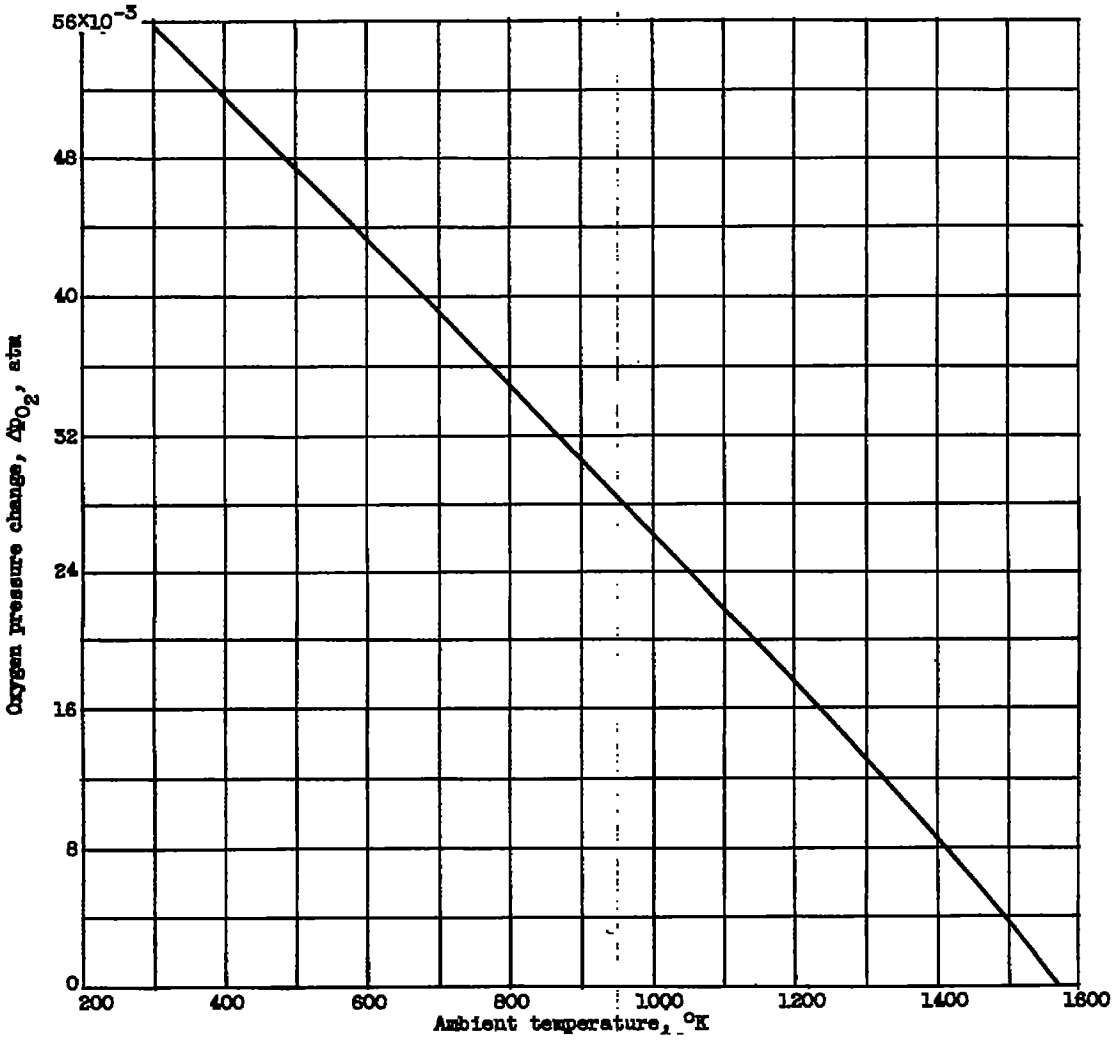


Figure 5. - Correction to ambient partial pressure of oxygen for departure of ambient temperature from 1570° K (eq. ($34_B$), appendix B).

4076

4076

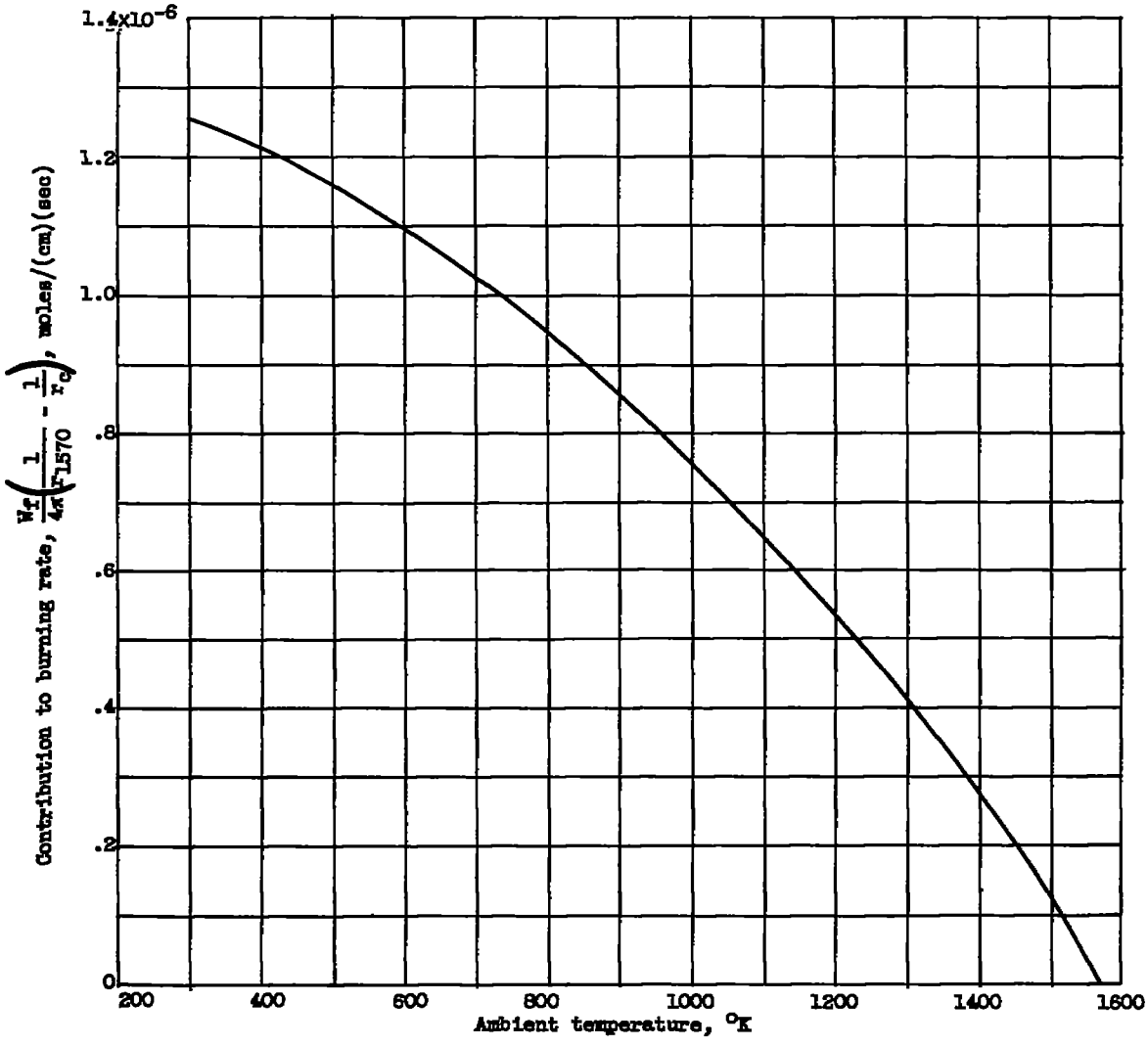


Figure 6. - Contribution to burning rate for ambient temperature below 1570° K (eq. ($36_B$), appendix B).

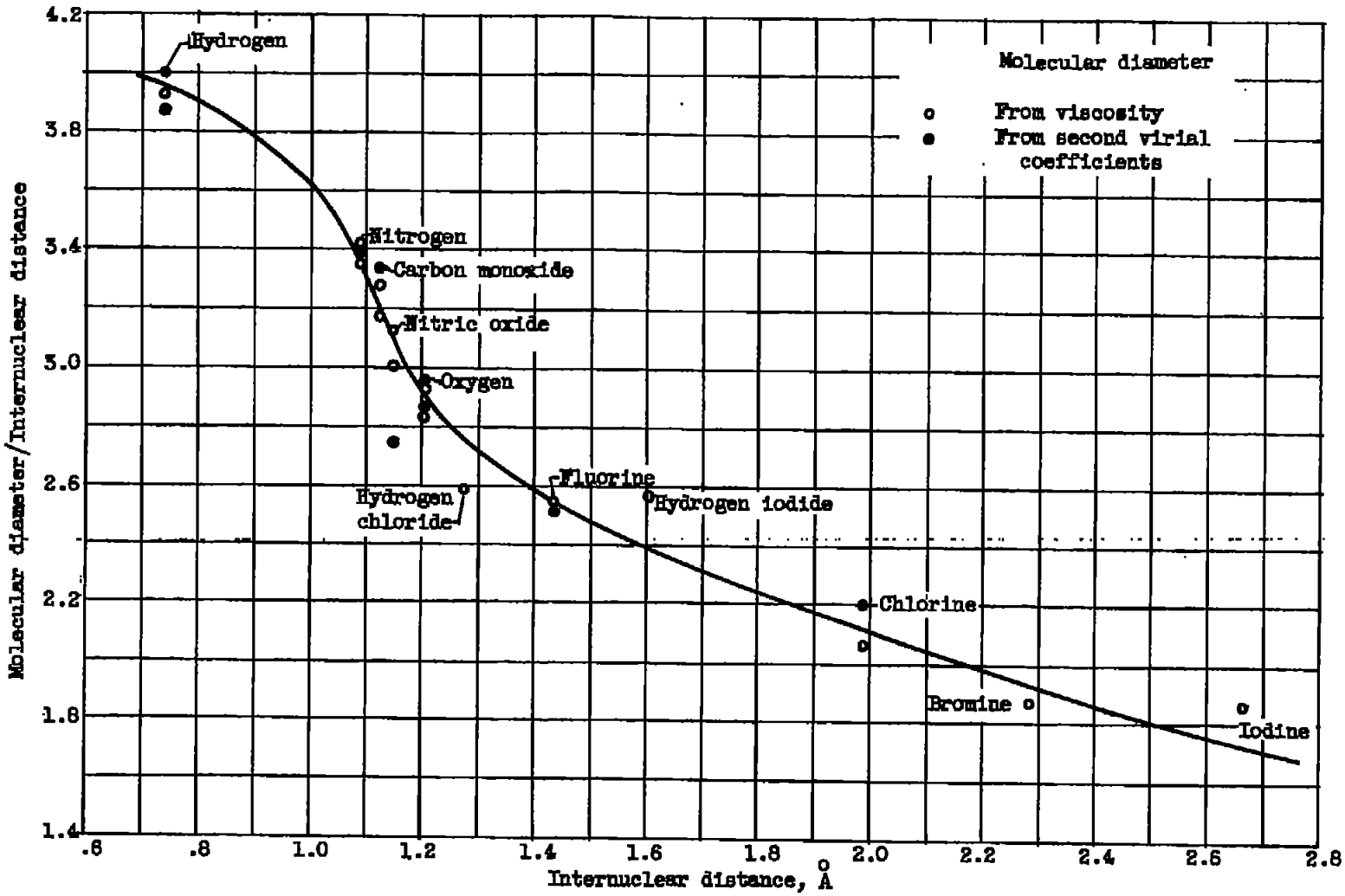


Figure 7. - Correlation between molecular diameter (ref. 10) and internuclear distance (ref. 12) for diatomic molecules.